AMERICAN UNIVERSITY OF BEIRUT

ANTENNA DESIGN FOR THE LEBANESE LINEAR PLASMA DEVICE

by
RAYAN ABBASS ALSAYED ALI

A thesis
submitted in partial fulfillment of the requirements
for the degree of Master of Engineering
to the Department of Electrical and Computer Engineering
of the Maroun Semaan Faculty of Engineering and Architecture
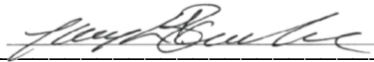at the American University of Beirut

Beirut, Lebanon
August 2020

AMERICAN UNIVERSITY OF BEIRUT

ANTENNA DESIGN FOR THE LEBANESE LINEAR PLASMA DEVICE
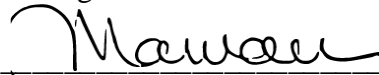
by

RAYAN ABBASS ALSAYED ALI

Approved by:

_____

Dr. Joseph Costantine, Associate Professor   Advisor
Electrical and Computer Engineering

_____

Dr. Ali Hajj, Professor   Member of Committee
Electrical and Computer Engineering

_____
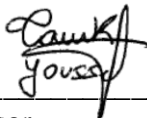
Dr. Marwan Darwish, Professor   Member of Committee
Mechannical Engineering

_____

Dr. Ghassan Antar, Professor   Member of Committee
Department of Physics

_____

Dr. Youssef Tawk, Assistant Professor   Member of Committee
Electrical and Computer Engineering

Date of thesis defense: [August 24th, 2020]

AMERICAN UNIVERSITY OF BEIRUT

THESIS, DISSERTATION, PROJECT RELEASE FORM

Student Name: _____Abbass_____AlSayed Ali_____Rayan_____
                             Last   First

          Middle

● Master's Thesis   ◯ Master's Project   ◯ Doctoral Dissertation

[ ]   I authorize the American University of Beirut to: (a) reproduce hard or electronic copies of my thesis, dissertation, or project; (b) include such copies in the archives and digital repositories of the University; and (c) make freely available such copies to third parties for research or educational purposes.

[X]   I authorize the American University of Beirut, to: (a) reproduce hard or electronic copies of it; (b) include such copies in the archives and digital repositories of the University; and (c) make freely available such copies to third parties for research or educational purposes
after:

        One ---- year from the date of submission of my thesis, dissertation, or project.
        Two ---- years from the date of submission of my thesis, dissertation, or project.
        (Three) ---- years from the date of submission of my thesis, dissertation, or project.

_____ _Rayan_ _____August 26th, 2020_____

Signature   Date

This form is signed when submitting the thesis, dissertation, or project to the University Libraries

ACKNOWLEDGMENTS

AN ABSTRACT OF THE THESIS OF

Rayan Abbass AlSayed Ali   for   <u>Master of Engineering</u>
<u>Major</u>: Electrical and Computer Engineering

Title: <u>Antenna Design for the Lebanese Linear Plasma Device</u>

Plasma, the fourth state of matter comprising almost 99% of the world, grabbed the attention of many researchers whose work referred basically to analyzing and understanding the characteristics and behavior of this state of matter. Due to their high efficiency in depositing electromagnetic power and producing dense plasma with high ionization degree, Helicon plasma sources have become extensively applied in basic research and for several applications. One of the major parts of a Helicon plasma device is the antenna responsible for coupling RF power into the plasma and driving the discharge. Thus, it is of high importance to investigate, analyze, and assess the performance of the employed RF antenna in order to maximize or optimize the power being deposited into the plasma. In our work, we conduct a comparative analysis among different antennas that are characterized by different properties such as; directivity, gain, input impedance, and others. This allows establishing a relationship between the properties of an antenna and its power deposition capabilities, and deducing what parameter enhancement generates denser plasma. This was followed by proposing a new antenna design with enhanced characteristics, capable of coupling energy more efficiently and generating denser plasma.

A comparative analysis is conducted among four different antenna structures that are commonly used in helicon plasma sources; namely, the anti-parallel double loop, the parallel double loop, the fractional helix, and the parallel fractional helix. These antennas are symmetrically wrapped around the plasma column of AUB's Lebanese Linear Plasma Device (Polaris), and tested in order to investigate and analyze the overall plasma profile of this plasma source. The investigative, theoretical and experimental work have shown that the parallel double loop antenna, which is the antenna with the highest gain value, generated plasma with the highest electron density. Hence, in order to correlate the gain enhancement with the improved energy coupling and higher density plasma generation, a new antenna design is proposed. The proposed design is a modified helix antenna that was designed and experimental validated. Once installed on Polaris, it attained an average electron density that is much greater than the average electron density value achieved by the parallel double loop antenna. This reassures the conclusion drawn in our comparative analysis, which states that antennas with higher realized gain values are the antennas capable of generating denser plasma.

CONTENTS

ILLUSTRATIONS

Figure

TABLES

CHAPTER I

INTRODUCTION

A. Background and Motivation

Plasma, the fourth state of matter comprising almost 99% of the world, grabbed the attention of many researchers whose work referred basically to analyzing and understanding the characteristics and behavior of this state of matter. The production of plasma using helicon plasma sources has proven to be highly efficient. Helicon plasma sources are capable of producing high- density plasmas with a high ionization degree, under various external control parameters [1]. Moreover, these sources are considered one of the promising plasma sources that are attractive for many applications such as, Space plasma modeling, nuclear fusion, gas lasers, materials processing, plasma acceleration, semiconductor manufacturing, material surface modification, laboratory research, and spacecraft propulsion [2].

One basic component of a helicon plasma is the Radio Frequency (RF) and antenna systems. These systems are composed of three major parts: the RF power supply, the impedance matching network, and the antenna. The antenna is the component responsible for coupling the RF power into the plasma and driving the discharge [4]. However, the mechanism upon which the RF power is coupled into the plasma was not completely understood by the researchers and remains partially unchartered and requires further understanding [3].

1

Plasma densities exceeding $10^{19} m^{-3}$ can be reached by employing antennas that are simple in geometry [4]. The literature is rich with helicon plasma sources employing various types of antennas such as; simple loop antenna [4], Nagoya type- III antenna [4], double half turn antenna [6], Boswell antenna [8], twisted Nagoya- III [4], helical antennas [16], double- saddle antenna [5], and spiral antenna [5].

It is intuitive that one important task that must be fulfilled when generating plasma, is to maximize or optimize the power being deposited into the plasma. This necessitates the assessment of the performance of the antenna employed in the helicon plasma source to drive the discharge [4]. Moreover, an optimum coupling of the RF power into the plasma requires a comparative analysis that compares the performance of different antenna structures as typical plasma parameters are being varied. In other words, it is important to find out which antenna structure performs best in maximizing the deposited power for a given set of plasma parameters. It is always the aim of researchers to attain as much high plasma densities as possible.

B. Thesis Structure

In this report, we start with an introduction about helicon plasma sources, then we proceed with an overview about the various types of antennas that are used in plasma generation. Such common antennas are reproduced first to identify their performance parameters and criteria. In addition, a new antenna structure is proposed in order to increase the efficiency of power coupling into the plasma discharges as well as the density of plasma itself. The proposed antenna structure is modeled, designed and measured around a helicon tube in order to evaluate its performance.

CHAPTER II

HELICON PLASMA SOURCES

A. Introduction

The ordinary states of matter found on earth are solid, liquid, and gas. However, the English physicist Sir William Crookes identified plasma as a fourth state of matter existing in the stars as well as in the space between them [21]. In general, when an ordinary gas is heated or electrified, its atoms are dissociated into positively and negatively charged particles called ions and electrons respectively as shown in Fig. 1. The resultant mixture of ions and electrons is referred to as plasma and its characteristics are significantly different from those of the ordinary gas from which it is produced.

Due to their high efficiency in depositing electromagnetic power and producing dense plasma with high ionization degree, helicon plasma sources have become extensively applied in basic research and for several applications [4]. Space plasma modeling, nuclear fusion, gas lasers, materials processing, plasma acceleration, semiconductor manufacturing, material surface modification, laboratory research, spacecraft propulsion, and many other applications rely on helicon wave discharges as prime candidates for plasma generation [5].
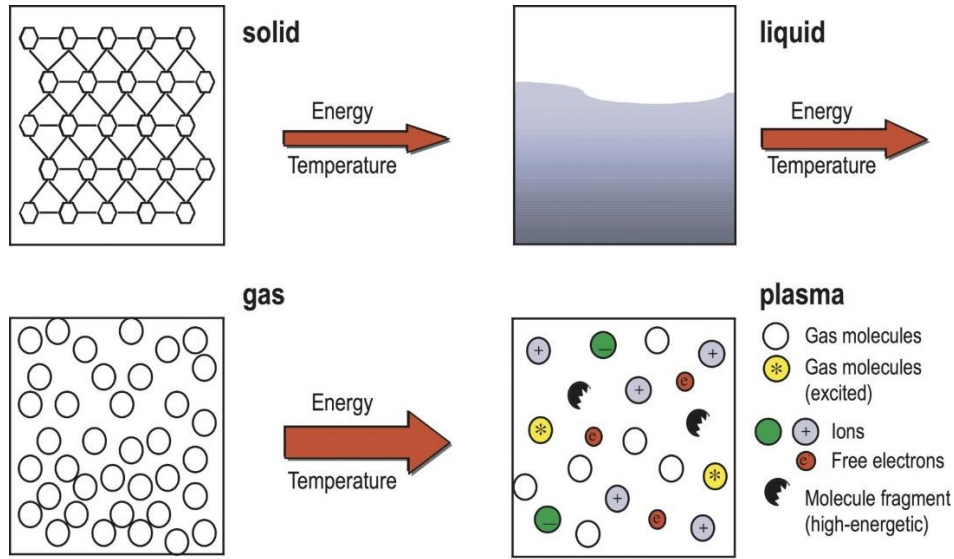
Figure 1: The Four States of Matter [22]

B. Literature Review

Helicon waves are categorized by researchers as whistler waves, which are right-hand circularly polarized electromagnetic waves in free space [23]. Despite the fact that theoretical studies and analysis of helicon plasma sources were initiated many years earlier, the first helicon plasma source was originated in an experiment conducted by Boswell in 1968 [3]. In his experiment, Boswell was capable of generating plasma densities as high as 10^{13} cm^{-3}, and obtaining the first blue core argon helicon plasma [3]. After the conduction of that first helicon plasma experiment, the number of journal publications hitting the topic of helicon plasma in the title or abstract has increased noticeably and the researchers seeking high density plasma sources, needed for a wide range of research experiments, rediscovered the helicon source [3].

Three distinct modes of operation are identified by Ellingboe and Boswell in [6], based on the RF magnetic fields measured in the near-field of the antenna employed in the plasma device. The three modes are labeled as capacitive (E- mode), inductive (H- mode), and helicon- wave mode (W- mode) [6]. Based on the measured plasma- wave- field profiles, the authors identify a dramatic change occurring at the transition from E to H mode, and another one occurring at the transition from H to W mode [6]. The two noticeable changes in the magnetic field profiles are referred to as "jumps".

In the E- mode of operation, the antenna imposes a magnetic field whose structure is not affected or modified by the plasma generated inside the cylindrical dielectric tube. Moreover, in the H- mode, the z- component of the field generated by the antenna is excluded from the bulk of the plasma. Also, in the W- mode, the measured plasma wave fields obey the dispersion relation of helicons [6].

Three types of plasma sources exist. These three types are summarized as: inductive, capacitive, or helicon. For the same RF input power, helicon sources clearly produce plasma with higher densities [7]. The primary intention when producing plasma is coupling the RF energy supplied by an external source into the center of a magneto-plasma and transferring this energy to the plasma particles [8]. However, the exact mechanism upon which the RF power is coupled into the plasma is not totally vivid. Researchers primarily explain the mechanism of RF power coupling by two different concepts: collisional and collision-less damping.

In 1985, Chen pointed out that the most convenient mechanism explaining the efficient energy absorption observed in helicon plasma sources is the collision- less damping, also known as Landau damping, because the interactions taking place between

5

the wave and the particles at the RF wave phase speed are capable of exciting the electrons' kinetic energies to a level equal to the ionization potential of argon [9]. On the contrary, some researchers believed that the helicon mode energy is transferred to the plasma electrons by collisional damping, in which the energy is transferred to the thermal electron population and the existing collisions cause a drag- on electron motion along the magnetic field, thus leading to the damping of the helicon waves [9]. After a deep investigation in the topic of ionization efficiency of helicon plasma sources, it became clear that neither the theory of collisional damping nor that of Landau damping could explain the results obtained by experiments [3].

A helicon plasma source is basically composed of three important sections: a cylindrical dielectric tube, coils, and an RF antenna system as shown in Fig. 3 [4]. The former part is responsible for the generation of the weak quasi-axial magneto- static field that allows both helicon wave propagation and plasma confinement inside the dielectric tube [4]. On the other hand, the RF antenna system is composed of an RF power supply feeding an antenna with RF energy through an impedance matching network. The employed antenna is responsible for coupling energy into the plasma and exciting the helicon waves.

C. Discussion

Helicon plasma sources are known to be the most efficient amongst other plasma sources. In a helicon plasma source, an antenna is the part responsible for generating waves capable of matching the wavelengths and polarizations of the helicon waves which are right handed circularly polarized waves present inside the plasma tube. This couples

energy into the plasma and drives the discharge. Energy absorption by plasma was referred by Chen in[9] to two mechanisms: Landau damping and collisional damping. Many antenna structures have been used in plasma generation, the most commonly known ones are the helical and helicon antennas.
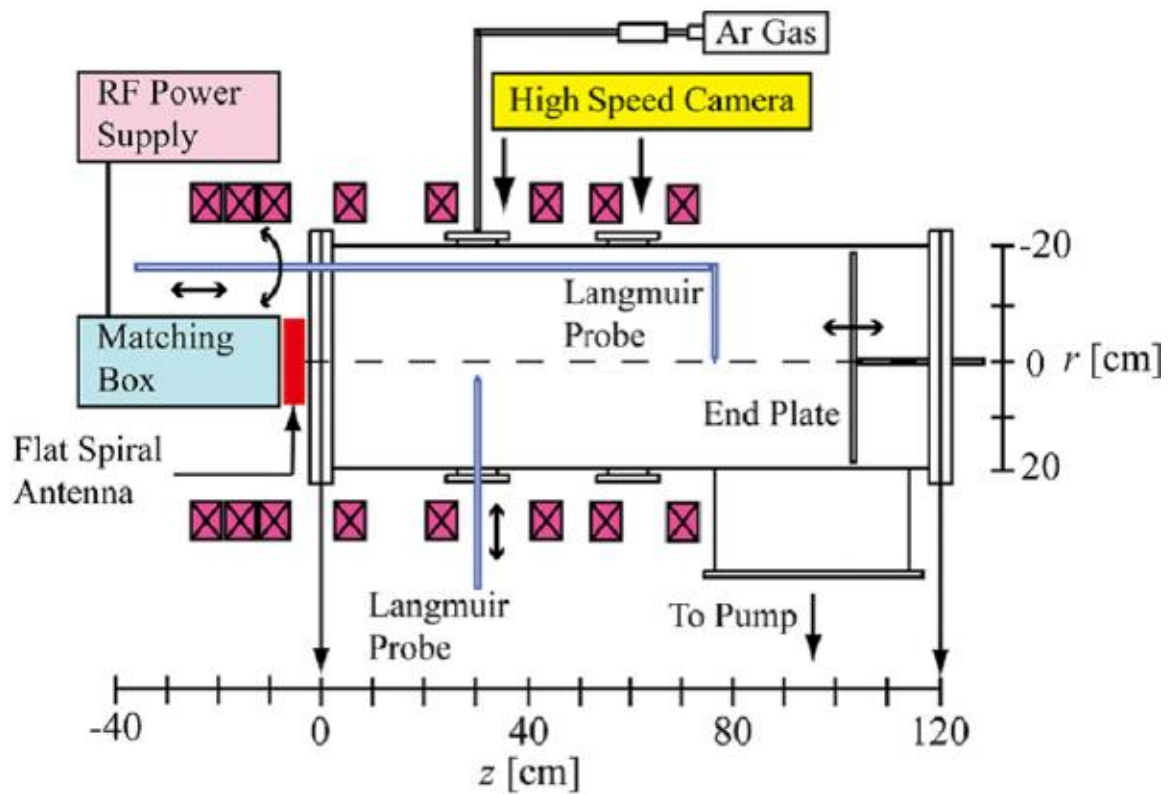
Figure 2: Schematic showing the main parts of a Helicon Plasma Source [1]

CHAPTER III

ANTENNAS USED IN HELICON PLASMA SOURCES

A. Introduction

High density plasma sources employ an antenna to couple energy, inductively, into the plasma [16]. Hence, one of the major parts of a helicon plasma device is the antenna [19]. The antenna surrounding the cylindrical dielectric tube operates in the frequency range $\Omega_{ci} \ll \omega_{lh} \ll \omega \ll \Omega_{ce}$, where Ω_{ci} and Ω_{ce} correspond to the ion and electron cyclotron angular frequencies respectively, and ω_{lh} resembles the lower hybrid frequency [4].

The antenna is designed in a way such that it is capable of exciting a spectrum of waves inside the plasma, which are characterized with wavelengths and field polarizations matching the expected wavelengths of the helicon waves present inside the system [5]. Therefore, accurate consideration of the antenna geometry in addition to the plasma parameters should be taken when designing a helicon plasma source, for the aim of achieving an efficient RF power coupling [2].

B. Literature Review

RF plasma generation, with the aid of a special driving antenna (Fig. 3) presented by Boswell in [8], was proven to be very efficient in helicon plasma sources [17]. This special antenna structure reported by Boswell, which is an antenna with no helical pitch, has been long used to aid the production of fully ionized plasma through coupling the

propagating waves into a whistler mode [8]. The Boswell antenna structure is shown in

Fig. 3.
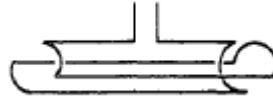
Figure 3: Boswell Antenna Structure [8]

Moreover, many antennas have been employed in order to excite the azimuthal

mode number m in the helicon wave scheme [18]. Researchers have investigated single-

and multi- loop antennas capable of exciting the $m = 0$ mode, Boswell type and double

saddle antennas capable of exciting $m = \pm 1$ modes simultaneously, rotating Nagoya

type- III antennas and antennas with a helical pitch that excite $m = 1$ or $m = -1$ in a

selective manner [18]. All of the above antennas are implemented into the helicon plasma

source by wounding them around an insulation tube characterized by a small radius. On

the other hand, the spiral antenna is used for a large diameter plasma where it is placed at

the end of the chamber through an insulation window [18].

Helical and helicon antennas are the most popular antennas that are routinely used

in plasma generation [16]. For a certain set of plasma parameters, the performance of the

antenna system is highly determined by the appropriate selection of the number of turns

and the type of helicon or helical antenna to be mounted on the plasma source [16].

Despite the fact that helical and helicon antennas are the primary types of antennas used

for helicon plasma generation, there are only few venues that compare their performance.

For this reason, the authors in [16] conduct a detailed analysis of various helices and

helicon antennas, and present the simulation data that allows a direct comparison among them.

Achieving an efficient RF power coupling, or in other words, maximizing the RF power deposited into the plasma is a requirement that necessitates assessing the performance of the antenna driving the discharge [4]. As a result, the authors in [4] present a comparative analysis among three helicon sources employing three different antennas, which are, the single loop, the Nagoya type-III, and the fractional helix as shown in Fig. 4 [4]. Due to the fact that the real part of the input impedance of the antenna resembles a measure of the antenna capability of coupling power into the plasma, the authors in [4] conducted their comparative analysis in terms of the input impedance and the induced current density.

One of the high-density helicon plasma sources is the Tokai Helicon Device [18]. This helicon plasma source employs a flat-type, segmented multi-loop antenna that is made up of azimuthally splitted segments [18]. Distributing these segments among four different radial positions enables the excitation of the azimuthal mode number m of $0, \pm 1, and \pm 2$ by solely choosing the proper feeder parts, i.e. by varying the electrical connections between the segments on the rear side of the antenna as shown in Fig. 5 [18]. The authors in [18] studied the performance of the generated plasma and the structure of the excited RF waves as per changing the azimuthal mode number.

Recently, researchers have put a recognizable effort to prove that employing a flat spiral antenna behind a quartz window, is capable of achieving a much higher plasma production efficiency in comparison to the efficiency achieved by the standard antenna configuration, when the antenna is wound around the quartz tube [1]. The advantage of

using a flat spiral antenna behind the quartz window of the helicon plasma source is that it reduces the aspect (axial length-to-diameter) ratio "A" of the plasma by reducing the axial length of the device [1]. This characteristic of plasma is particularly important for industrial and propulsion applications [7].
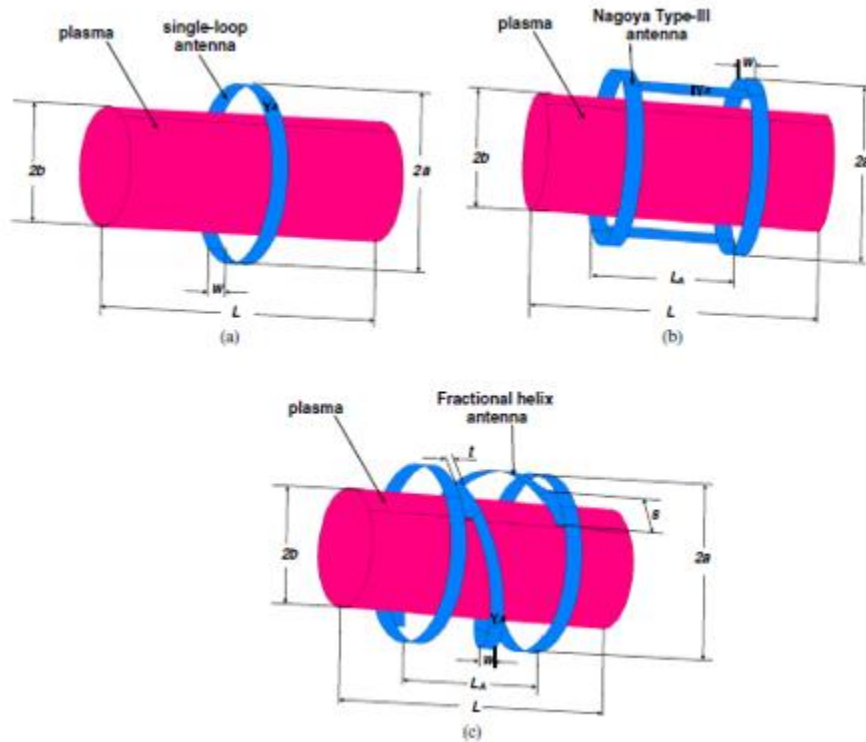
Figure 4: CAD models of the Helicon sources analyzed: (a) single loop, (b) Nagoya type-III, and (c) fractional helix [4]

The literature of plasma is rich with characteristics of helicon plasma sources at low or moderate RF powers (up to 2 kW). However, measurements and analysis at larger RF powers are few [20]. The Resonant Antenna Ion Device (RAID) is a helicon plasma device constructed for the purpose of investigating the functioning of helicon sources in a

11

new regime at which the steady-state operating power is 10kW (currently operating at 4 kW) [20]. This helps inferring the characteristics of helicon plasma sources at high operating RF powers.
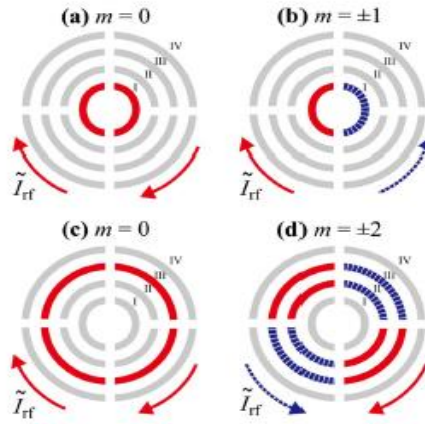
Figure 5: A schematic of RF antenna connections for the excitations of m = (a) 0 (the use of #I loop segments), (b) ± 1 (#I), (c) 0 (#III), and (d) ± 2 (#II and #III in a series connection) [16]

The multi-element antenna employed for power coupling is a unique RAID birdcage antenna as shown in Fig. 6 [20]. The birdcage resonant antenna is designed to accomplish the task of efficient RF power coupling to the $m = \pm 1$ helicon waves excited inside the plasma [20].
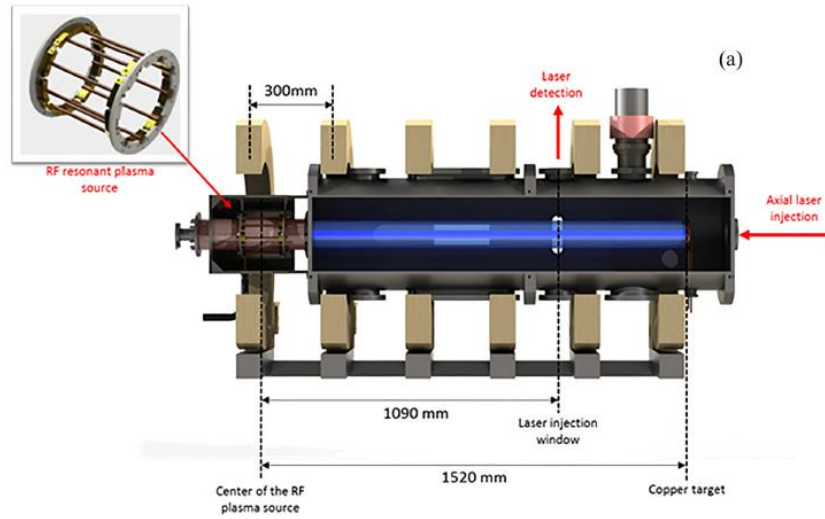
Figure 6: RAID schematic showing the unique, high-power, birdcage antenna [20]

The authors in [6] conduct measurements of the near-field magnetic field of a helicon plasma source, namely called WOMBAT, and identify three distinct modes of operation for this source: capacitive, inductive, and helicon-wave. The results they reported were conducted for a double- half- turn antenna (DHT) (Fig. 7), which has no current components in the direction parallel to the axial magnetic field [6].
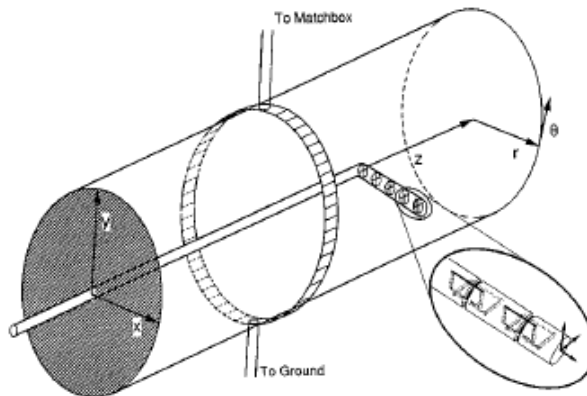
Figure 7: Schematic of WOMBAT source with the double-half turn antenna [6]

In addition to all of the RF antennas mentioned before, helical and helicon antennas are also basic antennas that are routinely used to inductively couple RF power into the plasma discharges [21]. However, it is always empirical to decide what type of helicon or helical antenna to use, and how many number of turns to select [16]. For this reasons, the analysis conducted by the authors in [16], was made among four cases of helices with number of turns N=1, 2, 3, and 4, as well as two helicon antennas, namely half and full Nagoya type antennas. It is shown from Fig. 8 the various modes that are exhibited by relying on various antenna types that are wrapped around the helicon tube. The authors conducted their comparative analysis by relying on 3D electromagnetic simulation and pointed out that for a constant current, as the number of turns N increases, the fields scale up and become more uniform [16]. Also, for the same current, Nagoya type antennas generate smaller fields compared to the fields generated by helical antennas.

Helix N=1

Helix N=2

Helix N=3

Helix N=4

Half-Nagoya type

Full Nagoya type
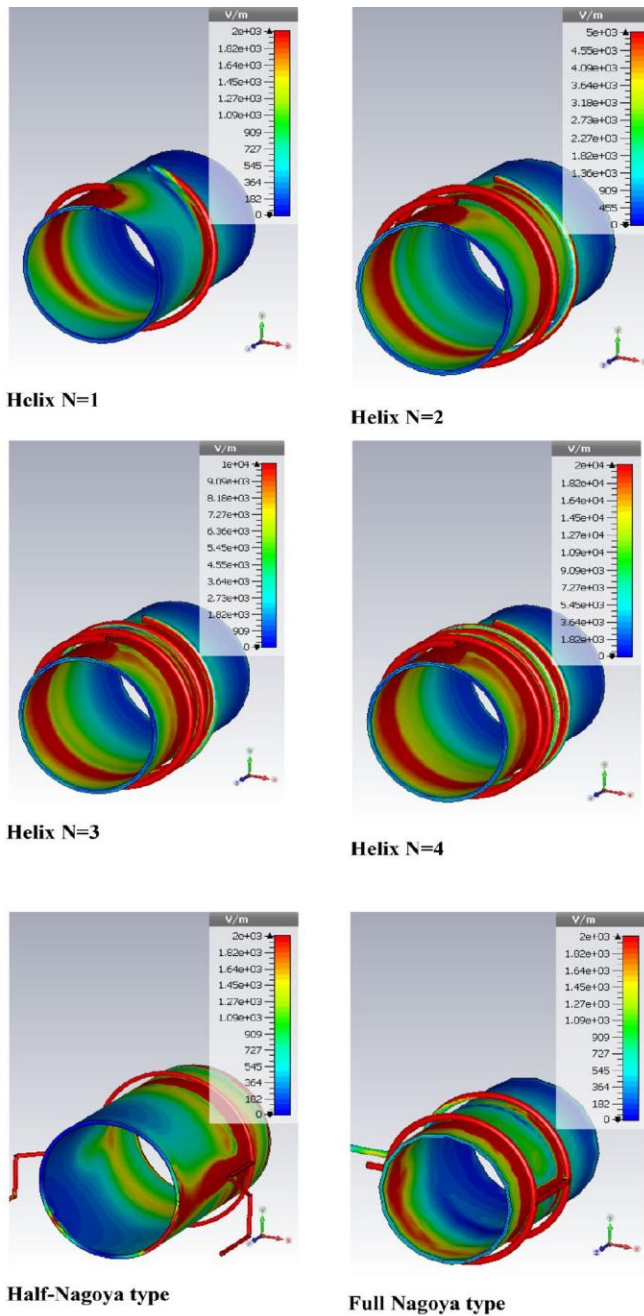
Figure 8: Electric field distributions on the surface of the dielectric cylinder surrounded by various helical and helicon antennas for the same current [16]

15

C. Antenna Modeling

In this part, the antennas designed and discussed in [4] are simulated and modeled. In fact, the authors in [4] compare amongst three different antenna structures that are employed in three different helicon plasma sources in order to drive the discharge. The three antenna types that are investigated are the single loop, Nagoya type-III, and the fractional helix antennas. The comparative analysis is based upon comparing the input impedance, which signals the antenna power coupling efficiency, and the distributed current density. These comparisons allow the identification of the antenna that performs best for a certain combination of plasma parameters, that is; maximizing the deposited power.

In their parametric study, the authors compare the performance of three different RF antennas with respect to the input impedance Z_A, while varying typical plasma parameters but keeping the size of the plasma column and the antennas fixed [4]. This criterion identifies which antenna outperforms the other two for a given set of discharge parameters. The set of plasma parameters analyzed constitutes of: plasma density, magnetostatic fields, neutral background pressure, and electron temperature. Each of these parameters is varied, and its effect on the antenna's input impedance and power deposition is analyzed. It is important to note here, that all of the three antennas are characterized with input impedances whose imaginary parts are positive, which ensures that the analyzed helicon sources are of an inductive nature.

Experimental Setup

The investigated helicon plasma sources comprise of the following key points:

- ✓ Circular cylindrical column, 10 cm long and with a radius $b = 2$ cm

- ✓ Argon plasma fills the cylindrical column

- ✓ The antenna is placed symmetrically around the center of the plasma column

- ✓ The radius of each of the antennas is a=3 cm

- ✓ The width of the metallic strips is $w = 0.6$ cm for the three antennas

- ✓ The length of the Nagoya and the fractional helix antennas is 5 cm

- ✓ The operational frequency is 15 MHz

- ✓ $V_G = 1\ V$ excites each antenna in the port region

The three antennas under investigation are reproduced and simulated by relying on Ansys' electronics desktop [24]. The simulation quantities that are desirable to be observed are the reflection coefficient parameter S_{11} and the gain of each of the analyzed antennas.

1. *Single Loop Antenna*

The antenna shown in Fig. 9 presents a single loop antenna that wound around a cylindrical vacuum tube. This tube mimics the position where the plasma is to be generated due to the loop antenna. The antenna is designed to operate at 15 MHz with radius a= 3cm. The antenna's circumference is chosen based on the dimensions of the both the cylindrical tube and the plasma device as a whole.
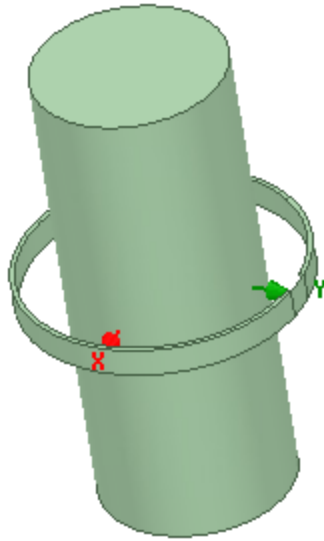
Figure 9: Single loop antenna
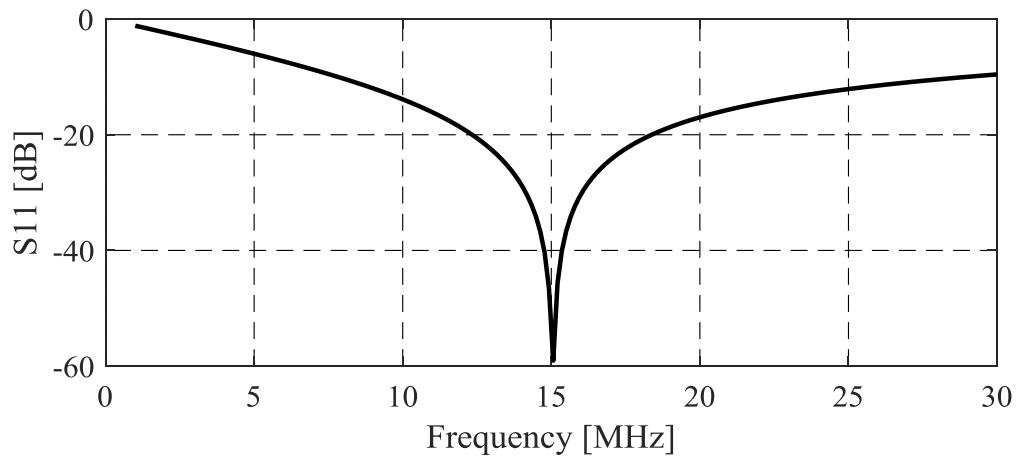
Figure 10:S11 parameter for the single loop antenna

The magnitude of the S11 parameter for the single loop antenna is much lower

than -10dB, that is; the antenna under investigation is well matched at its desired

frequency (15 MHz) as shown in Fig. 10. The gain achieved with such an antenna is -

39.45 dB as shown in Fig. 11. The antenna radiation pattern achieves its maximum at the

spatial positions Θ=90°, ϕ=90° and Θ=90°, ϕ=-90°.
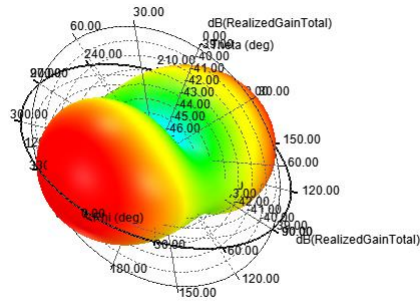
Figure 11: 3D gain plot for the single loop antenna

2. *Nagoya Type-III Antenna*

To enhance the gain of the antenna, two loops were joined to form the Nagoya type-III as

shown in Fig. 12.
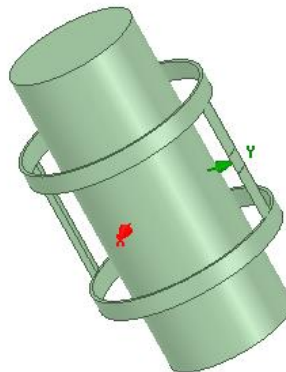
Figure 12: Nagoya type-III antenna

The magnitude of the S11 parameter for the Nagoya type-III antenna at the operational frequency f=15 MHz is significantly below -10 dB, which is an indication of the great impedance matching of the antenna as shown in Fig. 13. The gain achieved with such antenna is -29.19 dB which is higher than that of the single loop antenna as shown in Fig. 14. The antenna radiation pattern achieves its maximum at the spatial positions Θ=60º, φ=0º and Θ=120º, φ=180º.
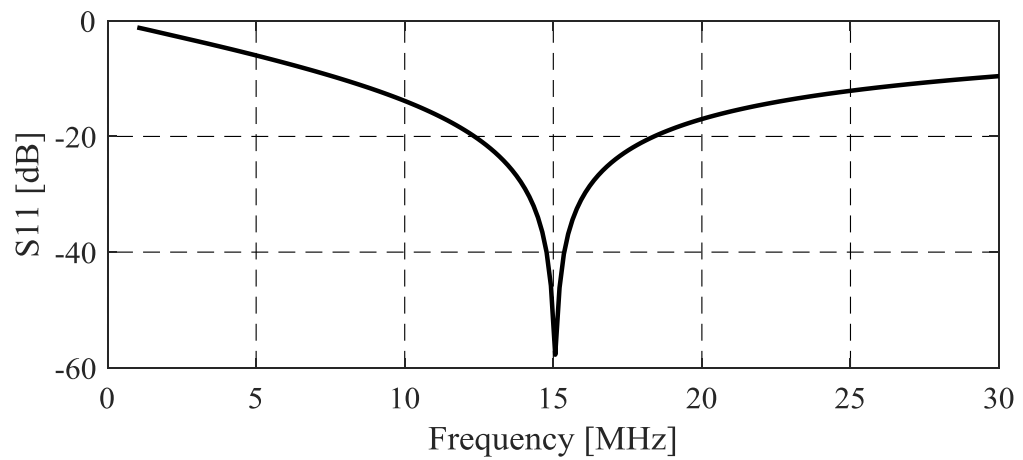
Figure 13: S11 parameter for the Nagoya type-III antenna
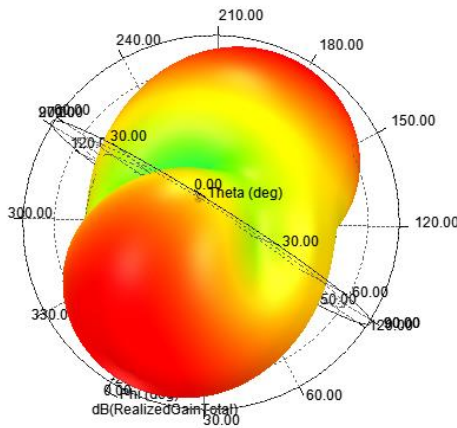
Figure 14: 3D gain plot for the Nagoya type-III antenna

20

3. Fractional Helix Antenna

In addition to the two modeled antennas a new antenna was investigated. This antenna also uses the two loops used in the structure of the Nagoya Type-III antenna; however, they are joined by two fractional helices instead of two straight strips as shown in Fig. 15. The fractional helix antenna is well matched at the operational frequency f=15 MHz, as shown in Fig. 16. The radiation pattern of the antenna is omnidirectional and it achieves a gain of -38 dB which is higher than that of the single loop antenna as shown in Fig. 17.
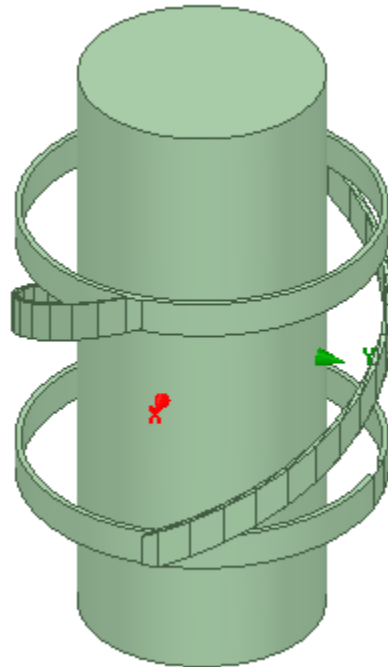
Figure 15: Fractional helix antenna
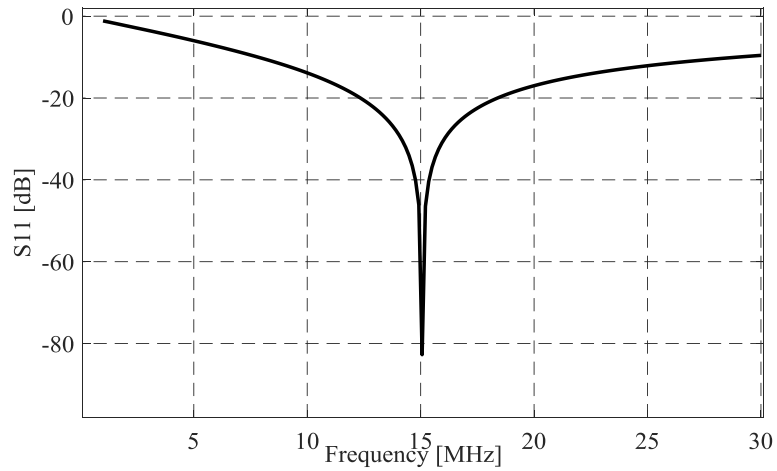
Figure 16: S11 parameter for the fractional helix antenna
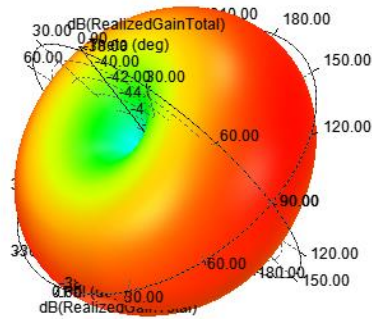
Figure 17: 3D gain plot for the fractional helix antenna

D. Conclusion

Helicon plasma sources have provided a good indication to be much more efficient, than other available plasma sources, at depositing power and producing dense plasma. A simple antenna structure can be employed in a helicon plasma source to attain plasma densities in the order of $10^{19} m^{-3}$ [4]. Thus, the RF antenna power system is an essential part of the helicon plasma source. The literature is rich with a wide range of

helicon plasma sources employing different RF antenna structures that are mostly wound around the cylindrical dielectric tube. In order to achieve high plasma densities, it is significant to maximize the power deposited into the plasma column. For this reason, researchers tend to evaluate and assess the performance of the antenna employed that is responsible of driving the discharge.

CHAPTER IV

COMMON ANTENNAS IN A LINEAR PLASMA DEVICE: FROM MODELING TO EXPERIMENTATION

A. Objective and Problem Statement

Being a major component of a helicon plasma device, the antenna responsible for coupling energy into the plasma should be designed with accurate consideration. Seeking an efficient power coupling by an antenna into plasma, necessitates a detailed investigation, analysis, and assessment of the RF antenna driving the discharge as a function of the changed plasma parameters. In order to maximize the power deposited into the plasma for the Lebanese linear plasma device, it is desired to conduct a comparative analysis among different antennas that are characterized by different properties such as; directivity, gain, input impedance, and others. This allows establishing a relationship between the properties of an antenna and its power deposition capabilities. The antennas to be compared will be mounted and tested experimentally on the Lebanese linear plasma device to investigate their characteristics and their influence on the efficiency of power coupling and generation of plasma.

RF plasma generation was conducted by several researchers with the aid of some antennas that became commonly used in the field of plasma. In this section, we model four different antenna structures, namely, the anti-parallel double loop, the parallel double loop, the fractional helix, and the parallel fractional helix. The modeling is followed by a detailed assessment of the performance of each of these antenna structures,

24

and a comparative analysis among the four antenna geometries in order to point out how to maximize the power deposited into the plasma.

Following the analysis part, four detailed experimentation setups are conducted using each of the modeled antenna geometries. The experiments are performed on the Lebanese Linear Plasma Device, known as "Polaris" plasma device, a helicon plasma source present in the plasma laboratory of the physics department at American University of Beirut. The helicon plasma device under experimentation comprises a 15cm long circular Pyrex cylindrical tube, filled with argon plasma and with radius a=2.5cm. Four different experimental runs are launched on the Polaris device. The four runs differ from each other for the structure of the antenna that will be wrapped symmetrically around the Pyrex tube.

For a more meaningful comparative analysis, the four antenna structures are kept as similar as possible, with the only difference being the geometrical shape configuration. The four antennas have a radius r= 3.5cm, and are symmetrically wrapped around the plasma column. For the four antennas, the width and height of the metallic rectangular strip are set to w= 3mm and h=1cm respectively, and the length of the structure is set to L=10cm. Finally, the operational frequency of the RF power supply is f=13.56 MHz, and the power supply's maximum limit is 2KW.

B. Modeling and Experimentation of Common Antennas

1. *Anti-Parallel Double Loop*

a. Simulation Data
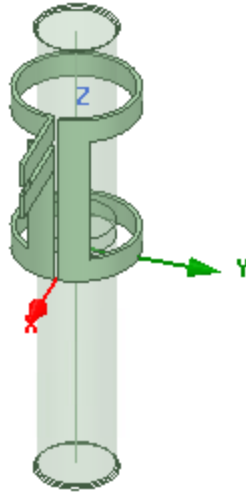
Figure 18: Anti-parallel double loop antenna

The Anti-parallel Nagoya antenna is modeled and simulated using HFSS, as shown in Fig.18, and the desired observable parameters are generated to verify the functionality of this antenna at the frequency of operation f=13.56 MHz
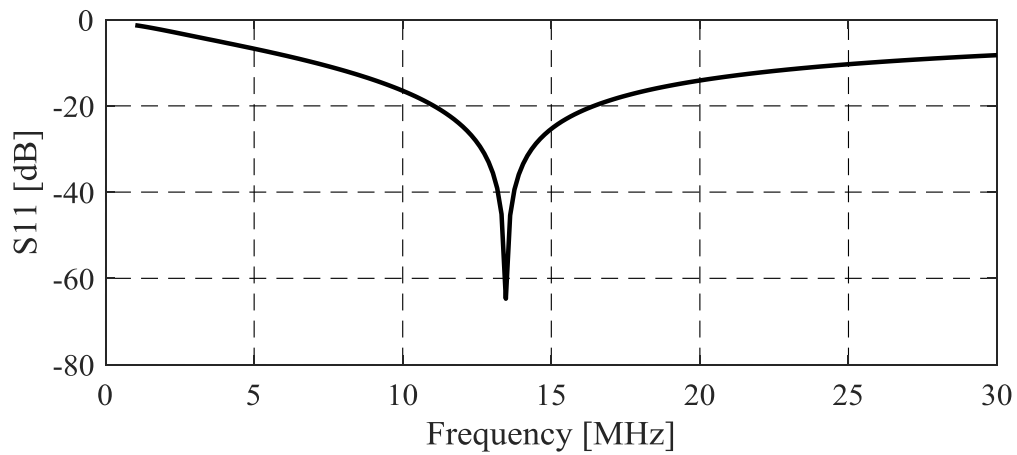
Figure 19: Reflection coefficient of the anti-parallel double loop antenna

The anti-parallel Nagoya antenna is well matched at 13.56 MHz as shown in Fig. 19. It is important to note here that the input impedance of the antenna 0.00+17.26jΩ, which is shown in Fig.20, will be matched to 50Ω, the impedance of the power supply, via a matching network placed between the RF power supply and the antenna.
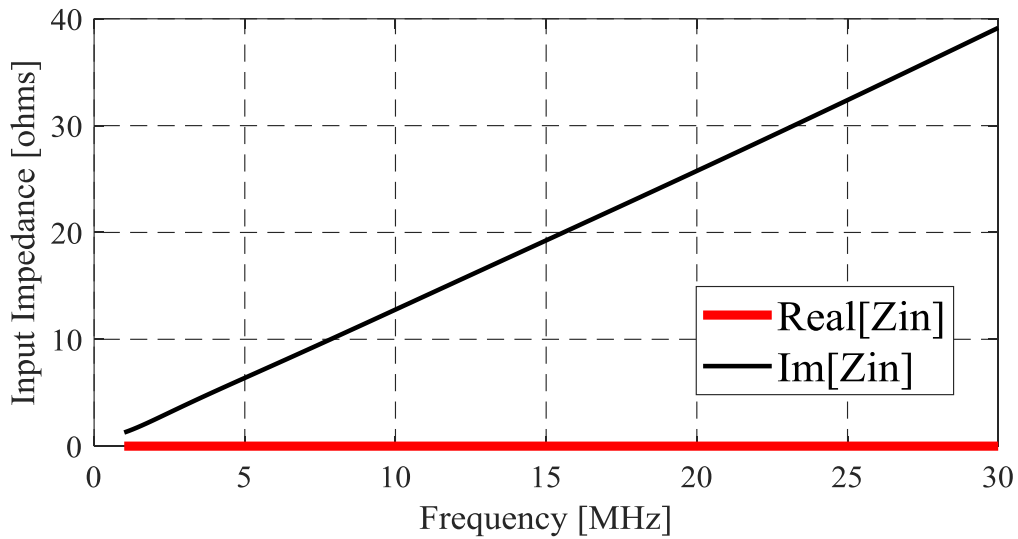
Figure 20: Input impedance of the anti-parallel double loop antenna

The 3D gain plot is shown in Fig.21. The radiation pattern of the anti-parallel Nagoya antenna design is a bi-directional pattern that has a maximum gain equal to -46 dB.
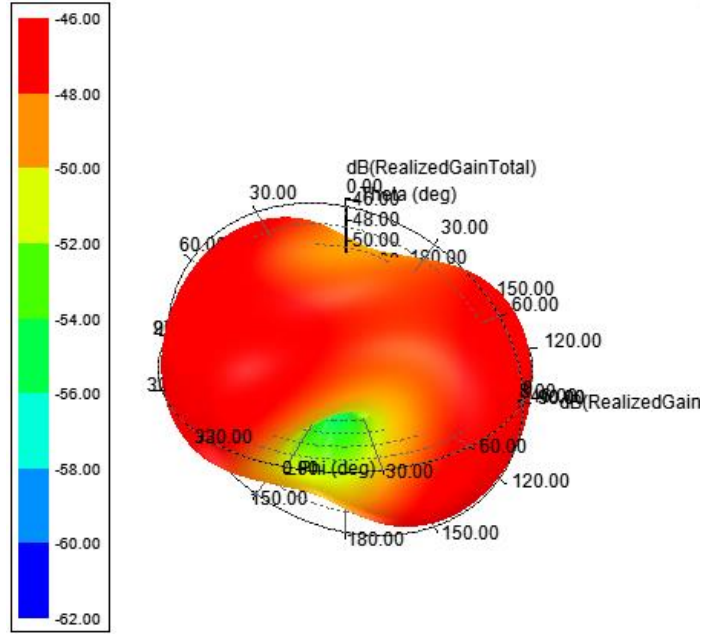
Figure 21: 3D gain plot for the anti-parallel double loop antenna

b. <u>Experimental Data</u>

The anti-parallel Nagoya antenna is modeled in 2D using cad tools, printed on a copper sheet of thickness 3mm, fabricated using conductive laser cutting techniques, and finally folded using a rounding machine. The fabricated structure is shown is Fig.22, and the direction of the propagating current is shown with white arrows.

Figure 22: Anti-parallel double loop fabricated structure

The testing of the anti-parallel Nagoya antenna, was performed at an external magnetic field B=300mT, and pressure P=2.21mT, with an argon gas flow of 13 SCCM. The experiment was repeated for six different runs, as shown in Table.4.1 below, all under the same external conditions except for the reflected power, which is the parameter that gives a measure of the mismatch between the impedance of the RF power supply and the antenna input impedance.

- P_{in}=1000 W
- B=300 mA
- P=2.21 mTorr
- Gas Flow= 13SCCM

Table 4.1: Experimental scans of the anti-parallel double loop antenna

RScan	P_{ref}(W)
1	13
2	75
3	125
4	156
5	200
6	270

The data acquisition tool, Langmuir probe, acquires the data throughout the experiment as voltages and the required parameters are found using Matlab. Fig.23 shows the electron density as a function of the radial position, inside the plasma column, for the anti-prallel Nagoya antenna. Each of the plotted curves corresponds to the scan acquired at a specific value of the reflected power.
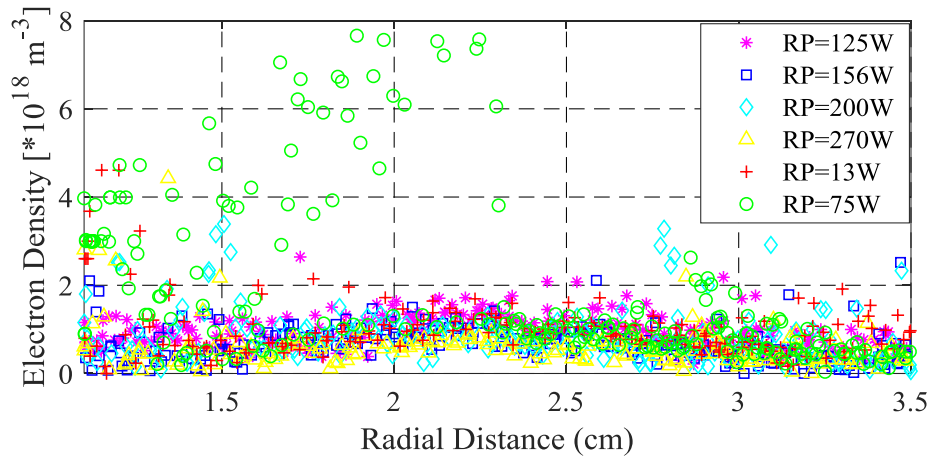
Figure 23: Electron density vs. radial distance for the anti-parallel double loop antenna

Fig.23 shows that under the best conditions; i.e. the reflected power is minimal (RP=13W), the average electron density attained inside the plasma column was $1.2764 \times 10^{18} m^{-3}$.

Fig.24 shows the electron temperature as a function of the radial position, inside the plasma column, generated by the anti-prallel Nagoya antenna. The figure plots the curves at six different reflected power values as shown in the plot legend.

As observed in Table. 4.1; six experimental scans were acquired for the anti-parallel Nagoya antenna. Each scan corresponds to a different value of the reflected power at the power supply. The reflected power is a measure of the mismatch between the source impedance and the antenna input impedance. Thus, it is of high importance to us, to see how the electron density and temperature change with the change in reflected power. In other words, we need to notice how mismatching the driving antenna to the source affects the density and temperature of the plasma generated inside the Pyrex column.

In order to accomplish this task; three main steps were taken. First, for each value of the reflected power; the electron density at each radial position is obtained. Second, the electron density values corresponding to radial positions falling between 2cm and 2.3cm are averaged to obtain one single value 'average electron density' at each reflected power value. Finally, a curve plotting the six reflected power values with their corresponding average electron density values is generated, as shown in Fig.46, at the end of this section.
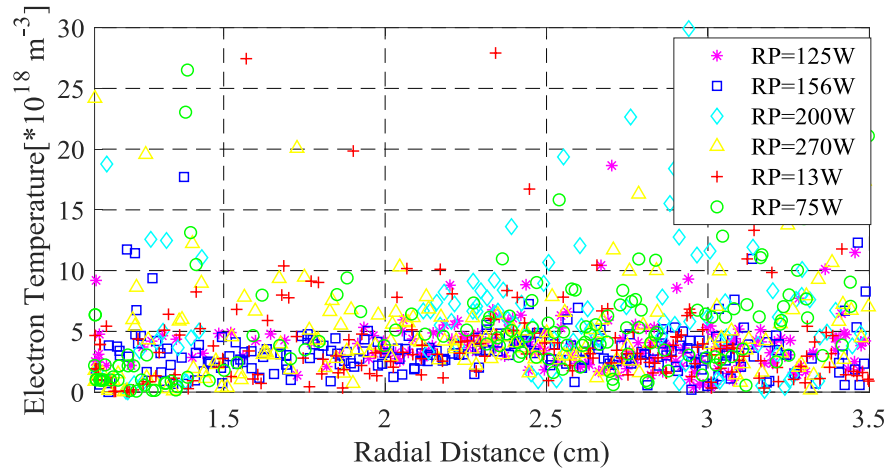
Figure 24: Electron temperature vs. radial distance for the anti-parallel double loop antenna

2. *Parallel Double Loop*

a. <u>Simulation Data</u>

Using Ansys Electronics Desktop; the parallel Nagoya antenna structure is modeled and simulated, as shown in Fig. 25.
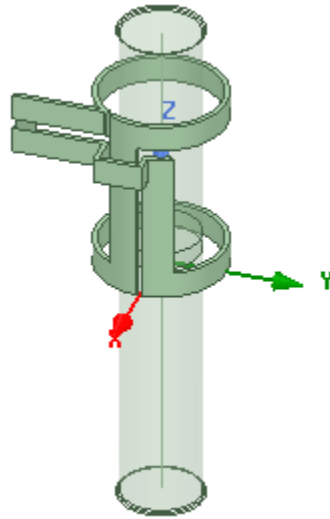
Figure 25: Parallel double loop antenna

The parallel Nagoya antenna is well matched at the frequency of operation f=13.6 MHz as shown in Fig.26.

The parallel Nagoya antennas is connected to the RF power supply through an impedance matching network responsible for converting the antenna input impedance, which is equal to 0.00+19.29i Ω as shown in Fig.27, to the source impedance, which is equal to 50 Ω.

Fig.28 below shows the 3D gain plot of the parallel Nagoya antenna. The radiation pattern of this antenna structure is bi-directional and has a maximum gain equal to -30 dB.

Figure 26: Reflection coefficient of the parallel double loop antenna
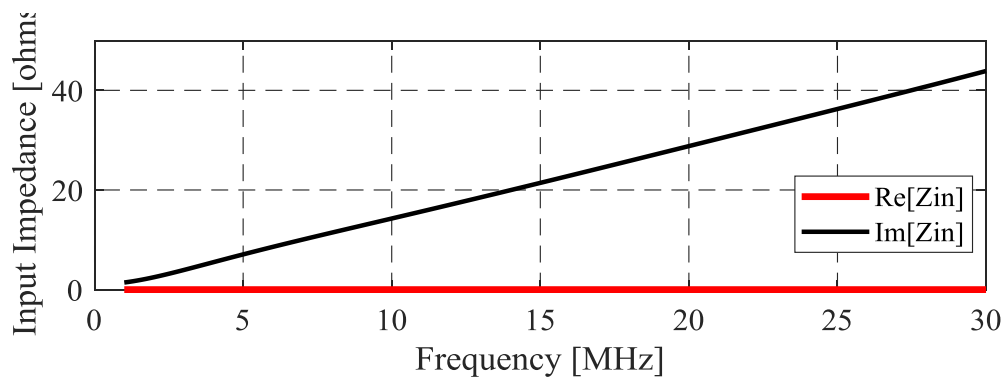
Figure 27: Input Impedance of the parallel double loop antenna
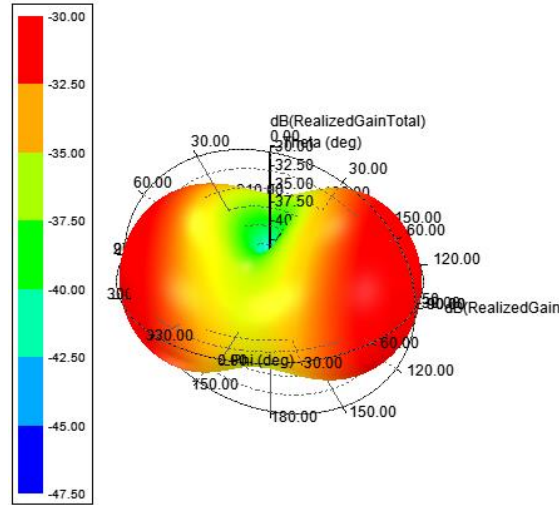
Figure 28: 3D gain plot for the parallel double loop antenna

b. Underline Experimental Data

The fabrication of the structure of the parallel Nagoya antenna was done using the exact procedure followed to fabricate the anti-parallel Nagoya geometry. The resulting design is shown in Fig.29.

Figure 29: Parallel double loop fabricated antenna

The testing of the parallel Nagoya antenna, was performed at an external magnetic field B=250mT, and pressure P=2.24mT, with an argon gas flow of 17 SCCM. Seven different runs were conducted, as shown in the Table.4.2, all under the same external conditions except for the reflected power, which varied increasingly from 20W in the first run to 300W in the final run.

- P_{in}=1000 W
- B=250 mA

Table 4.2: Experimental scans of the parallel double loop antenna

RScan	P(mTorr)	Gas Flow(SCCM)	P_{ref}(W)
1	2.24	17	20
2	2.24	17	65
3	2.24	17	125
4	2.31	17	150
5	2.31	17	200
6	2.21	16	250
7	2.21	16	300

Following the exact analytical procedure used for the anti- parallel Nagoya antenna structure, Fig.30 and Fig.31 show seven different plots of the parallel double loop antenna, each corresponding to a different value of the reflected power at which data was acquired, of the electron density and electron temperature respectively, as a function of the radial position, inside the plasma column.

Figure 30: Electron density vs. radial distance for the parallel double loop antenna
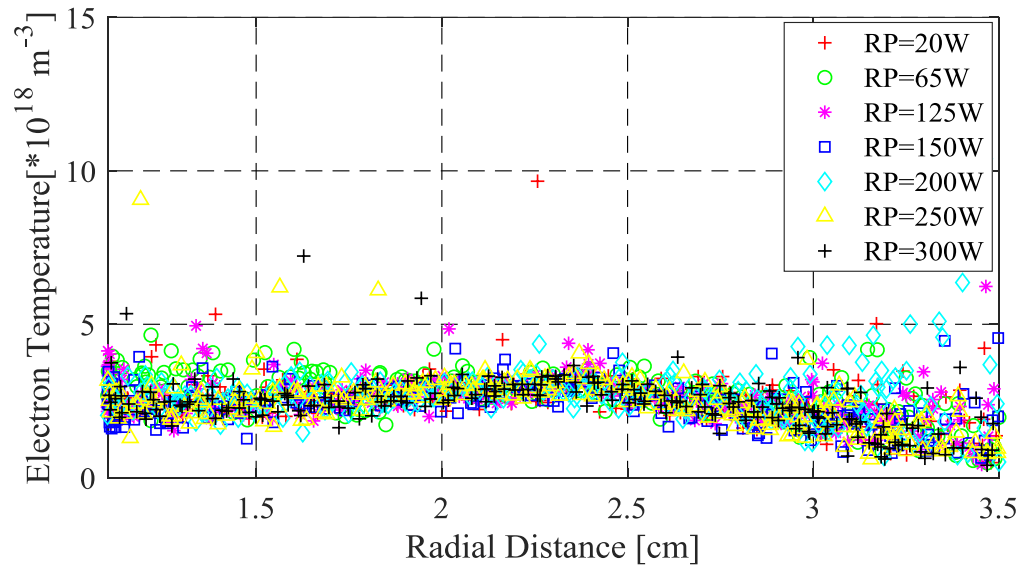
Figure 31: Electron temperature vs. radial distance for the parallel double loop antenna

The analytical procedure followed for the anti-parallel Nagoya antenna is repeated here, and the plot corresponding to the average electron density as a function of the reflected power is shown in Fig.46, at the end of section 4.

3. *Fractional Helix*

a. <u>Simulation Data</u>

Using Ansys Electronics Desktop; the fractional helix antenna structure is modeled and simulated, as shown in Fig. 32. The fractional helix antenna is well matched at the frequency f=13.56 MHz as shown in Fig.33. The fractional helix antenna is characterized with an input impedance 0.00+11.85 Ω, as shown in Fig. 34.

Figure 32: Fractional helix antenna

Figure 33: Reflection coefficient of the fractional helix antenna

Figure 34: Input impedance of the fractional helix antenna

Fig.35 below shows the 3D gain plot of the fractional helix antenna. The radiation pattern of this antenna structure is bi-directional and has a maximum gain equal to -37 dB.
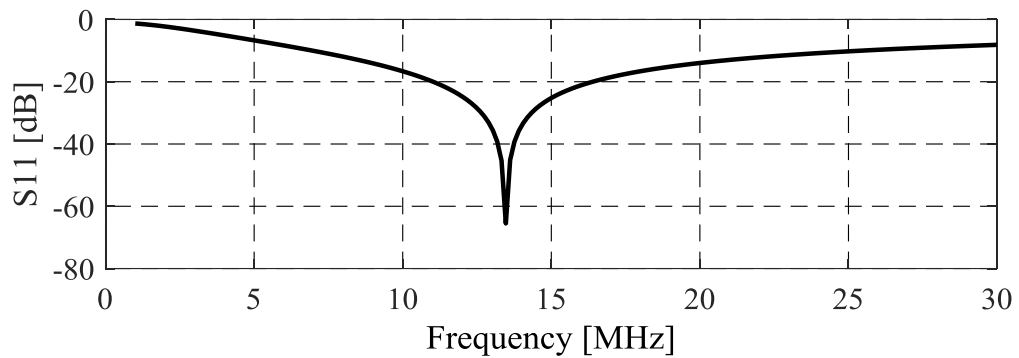
Figure 35: 3D gain plot for the fractional helix antenna

b. Experimental Data

The testing of the fractional helix antenna, shown in Fig.36, was performed at an external magnetic field B=250mT, and pressure P=2.37mT, with an argon gas flow of 18 SCCM. Nine different runs were conducted, as shown in Table.4.3, all under the same external conditions except for the reflected power, which varied increasingly from 9W in the first run to 260W in the final run.

Figure 36: Fractional helix fabricated antenna

- P_{in}=1000 W
- B=250 mA

Table 4.3: Experimental scans of the fractional helix antenna

RScan	P(mTorr)	Gas Flow(SCCM)	P_{ref}(W)
1	2.37	18	9
2	2.37	18	20
3	2.37	18	43
4	2.37	18	60
5	2.37	18	80
6	2.31	18	120
7	2.31	18	150
8	2.35	15	200
9	2.32	14	260

Following the exact analytical procedure used for the previous antenna structures, Fig.37 and Fig.38 show nine different plots of the fractional helix antenna, each corresponding to a different value of the reflected power at which data was acquired, of the electron density and electron temperature respectively, as a function of the radial

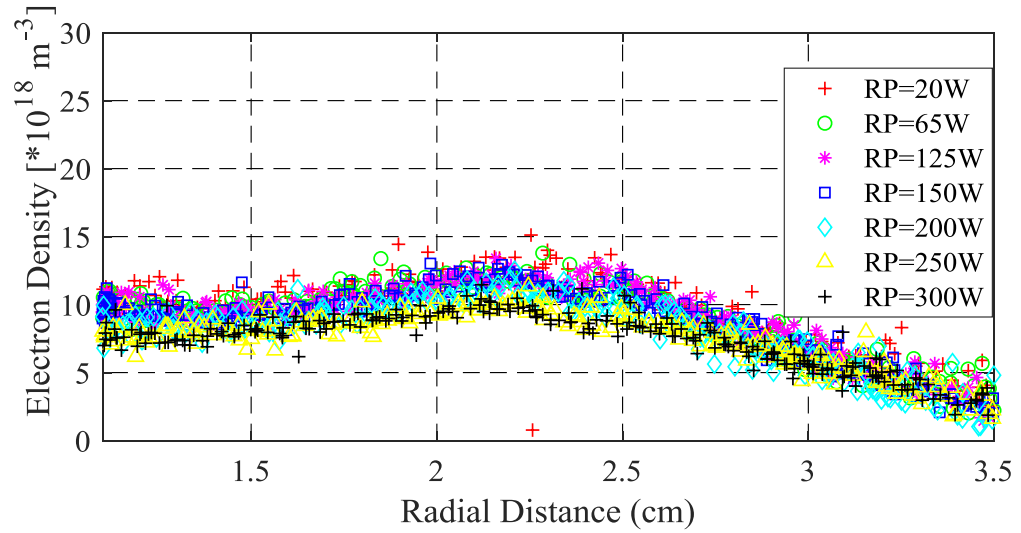position, inside the plasma column. The plot corresponding to the average electron density as a function of the reflected power is shown in Fig.46, at the end of section 4.

Figure 37: Electron density vs. radial distance for the fractional helix antenna

Figure 38: Electron temperature vs. radial distance for the fractional helix antenna

4. *Parallel Fractional Helix*

a. <u>Simulation Data</u>

Using Ansys Elecrtronics Desktop; the parallel fractional helix antenna structure is modeled and simulated, as shown in Fig. 39. The parallel fractional helix antenna is well matched at the frequency of operation f=13.56 MHz, as shown in Fig.40. The parallel fractional helix antenna is characterized with an input impedance $0.00+20.43i$ Ω, as shown in Fig. 41.
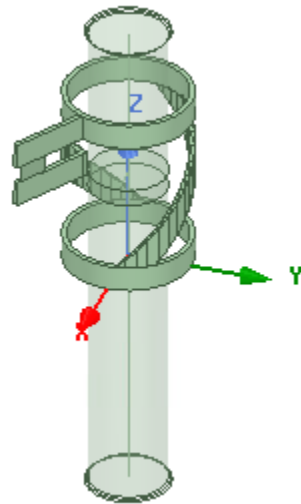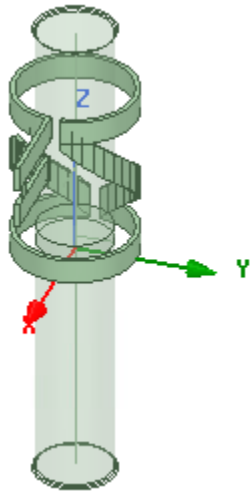

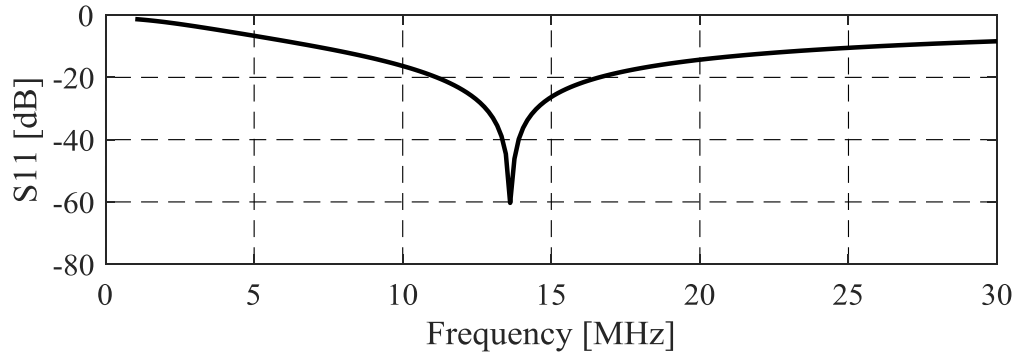Figure 39: Parallel fractional helix antenna
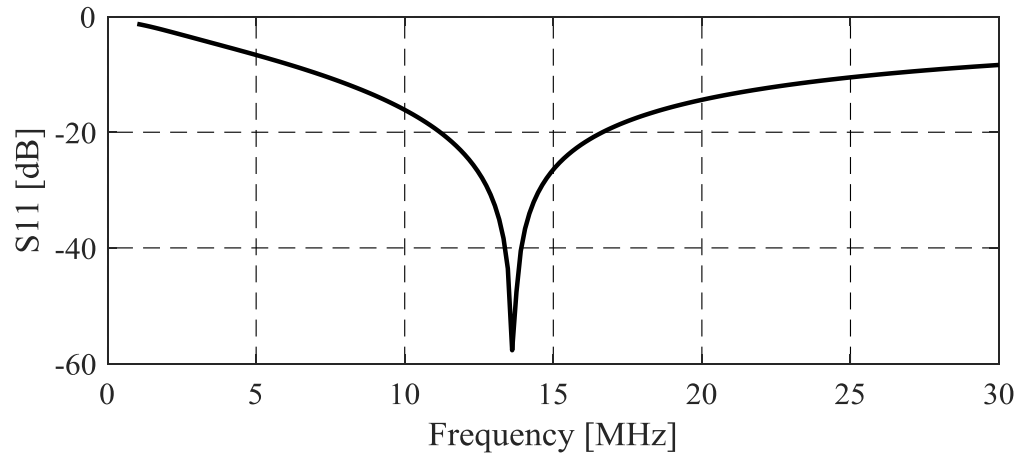
Figure 40: Reflection coefficient of the parallel fractional helix antenna
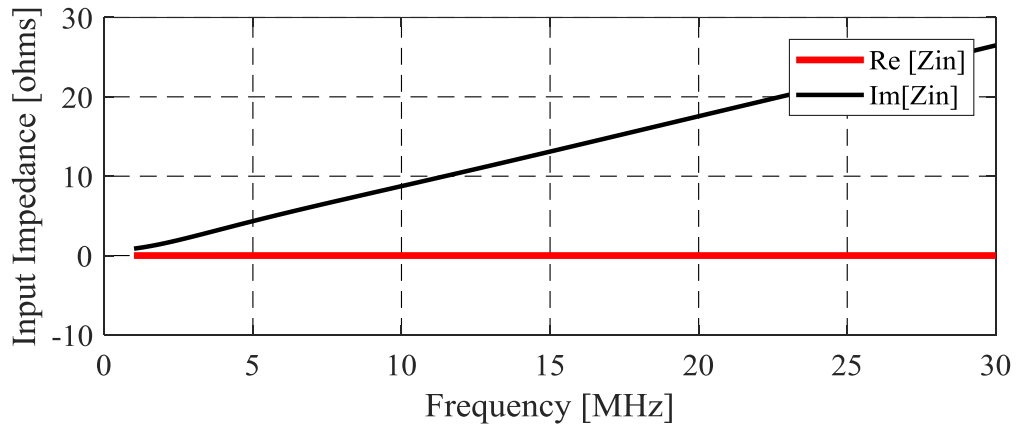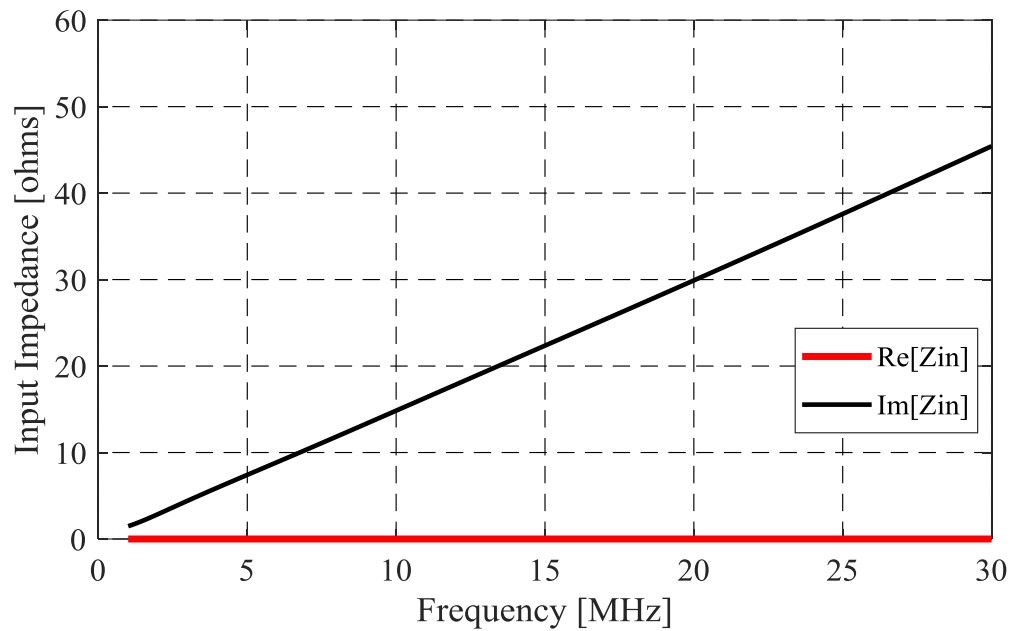

Figure 41: Input impedance of the parallel fractional helix antenna

Fig.42 below shows the 3D gain plot of the parallel fractional helix antenna. The radiation pattern of this antenna structure is bi-directional and has a maximum gain equal to -33 dB.
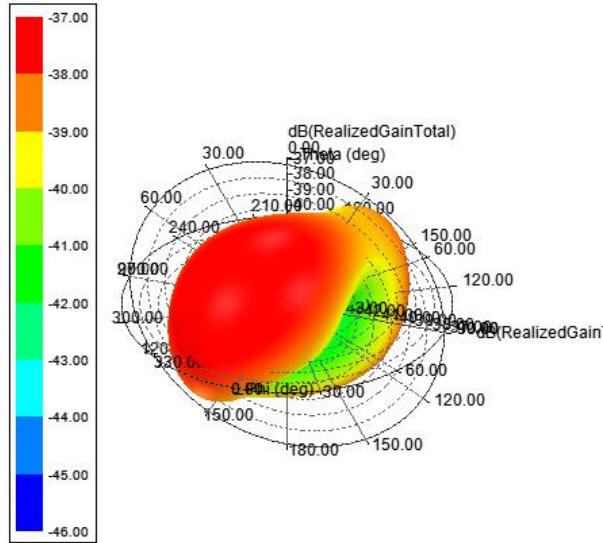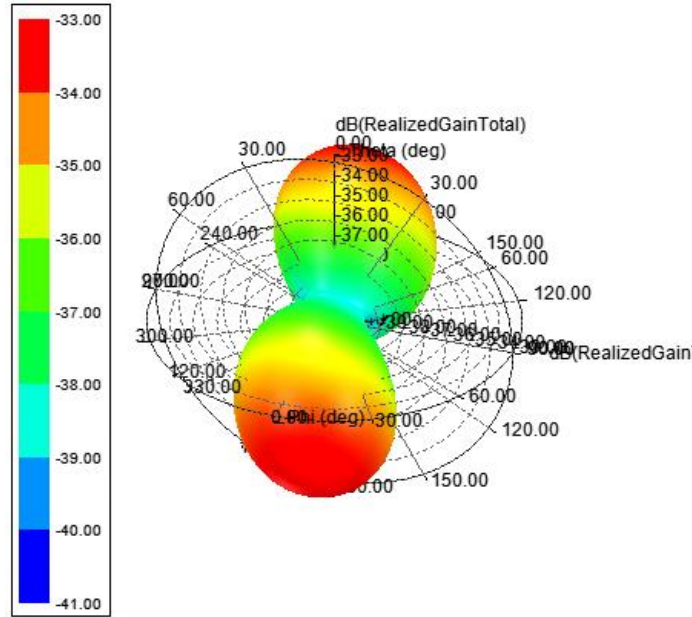
Figure 42: 3D gain plot for the parallel fractional helix antenna

b. <u>Experimental Data</u>

The testing of the fractional helix antenna, shown in Fig.43, was performed under the external condition shown in Table.4.4.

Figure 43: Parallel fractional helix fabricated antenna

- P_{in}=1000 W
- B=300 mA

Table 4.4: Experimental scans of the parallel fractional helix antenna

RScan	P(mTorr)	Gas Flow(SCCM)	P_{ref}(W)
1	2.28	18	7
2	2.28	18	16
3	2.28	18	30
4	2.28	18	50
5	2.28	18	75
6	2.28	18	110
7	2.28	18	160
8	2.21	16	180
9	2.26	16	240

Following the exact analytical procedure used for the previous antenna structures, Fig.44 and Fig.45 show nine different plots of the parallel fractional helix antenna, each corresponding to a different value of the reflected power at which data was acquired, of the electron density and electron temperature respectively, as a function of the radial position, inside the plasma column. The plot corresponding to the average electron density as a function of the reflected power is shown in Fig.46.
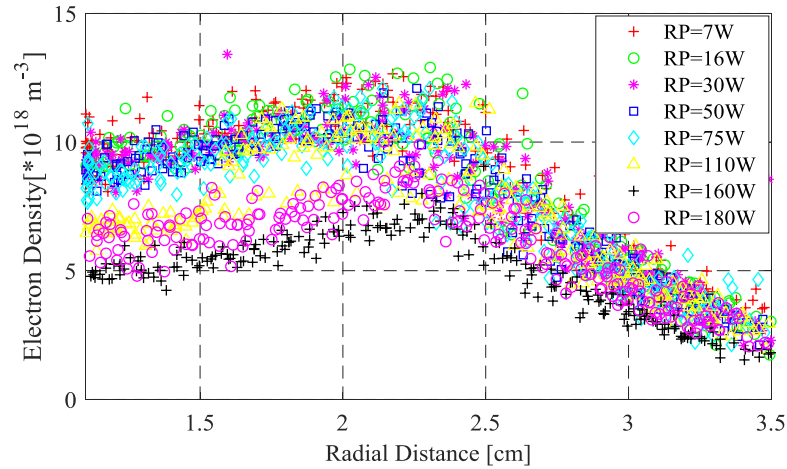
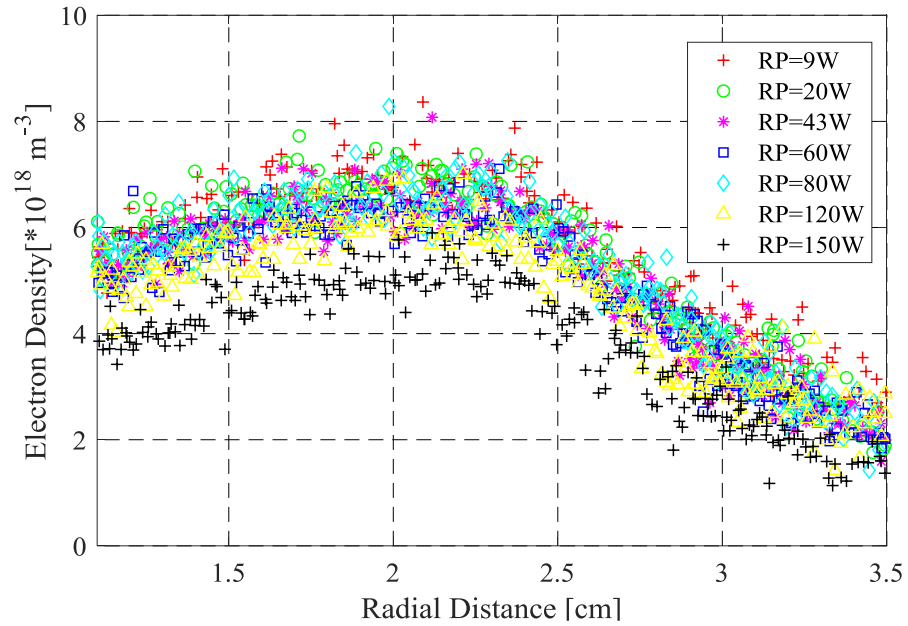Figure 44: Electron density vs. radial distance for the parallel fractional helix antenna

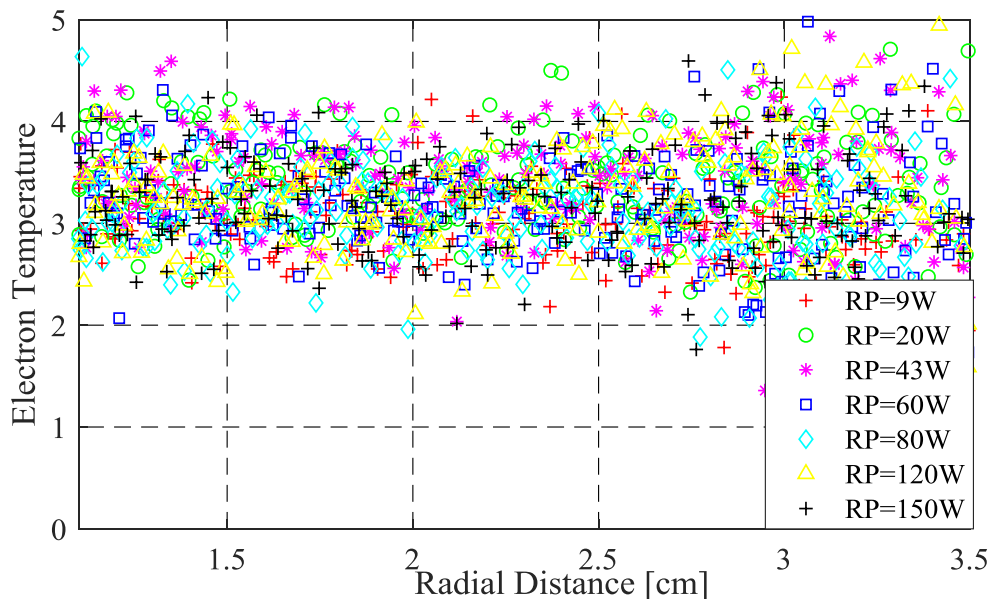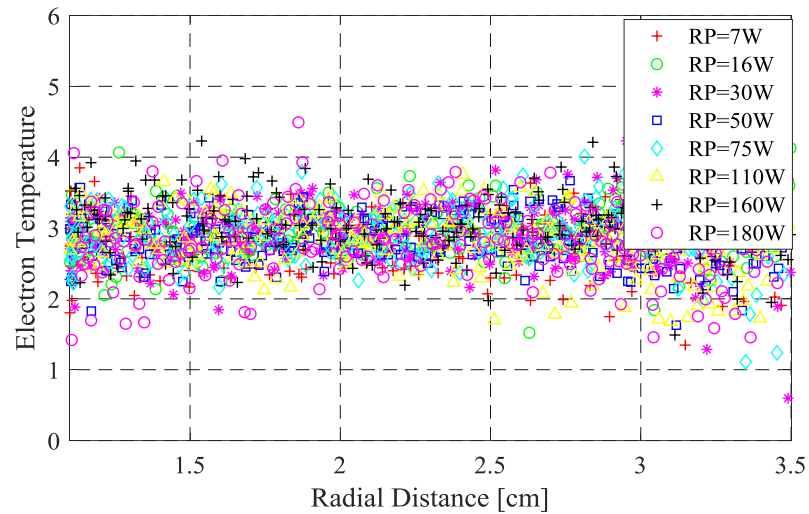Figure 45: Electron temperature vs. radial distance for the parallel fractional helix antenna

Fig. 46 shows the average electron density as a function of the reflected power for the four antenna configurations amongst which our comparative analysis is conducted. This plot was generated after acquiring multi experimental scans for each design at different values of reflected powers. It is clear from Fig. 47, that for all the four antennas under

investigation, and under whatever external conditions, the electron density values attained inside the plasma column are the highest when the antenna input impedance is perfectly matched to the source impedance which is equal to 50 Ω in our experiments, that is, the power deposited into the plasma column is maximal and the power reflected back to the source is minimal. As the driving antenna gets mismatched to the power supply, the reflected power starts to increase and the power deposited into the plasma column starts to decrease resulting in a lower electron densities inside the Pyrex tube. It is important to note here that our attempt to increase the reflected power was done by manually tuning the two variable vacuum capacitors, namely the tuning and loading capacitors, this modifies the state of matching between the driving antenna and the power supply and thus varies the amount of power driven into the plasma tube.
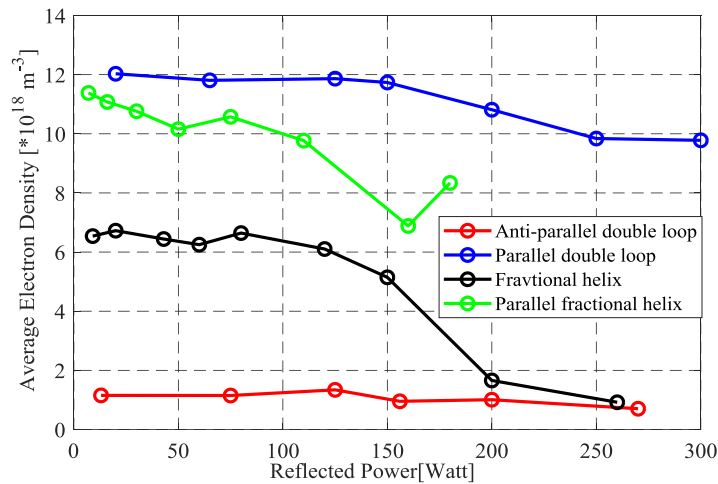
Figure 46: Average electron density vs. reflected power for the four antennas under investigation.

C. **Discussion and Comparison**

Table.4.5 summarizes the realized gain values attained by each of the four antenna geometries under investigation. The parallel double loop has the highest realized gain value of -30 dB, followed by the parallel fractional helix with -33 dB, then the fractional helix with -37 dB gain, and finally the anti-parallel double loop with the lowest gain value -46 dB. In addition, Table. 4.5 summarizes the input impedances of the four simulated antenna structures. In addition, it is significant to point out, that the positive imaginary part of the antenna's input impedance confirms the fact that the employed antenna couples the RF power inductively into the plasma. In experimentation, the input impedance of the antenna mounted on a helicon plasma device is converted to the impedance of the power supply, via a matching network placed between the RF power supply and the antenna. Moreover, the E-field, H-field, and maximum near E-field patterns are generated for the four antenna structures, and the maximum values attained are also summarized in Table. 4.6. These parameters are generated in order to point out which antenna characteristic correlates to the power coupling capabilities and plasma generation.

In reference to Chen's paper [24], two elements contribute to the value of the energy per unit volume, also referred to as energy density and expressed in J/m^3, these two elements are expressed in the following relation:

$$P_r = \frac{1}{2}\left(\varepsilon_0 E^2 + \frac{1}{\mu_0}B\wedge 2\right) \qquad (J/m^3)$$

What was clearly pointed out by the author in [24] is that the magnetic field has a much greater effect on the value of the energy density due to the fact that its magnitude squared is much larger than that of the electric field;

$$\frac{1}{2\mu_0}B^2 >> \frac{1}{2}\varepsilon_0 E^2$$

Table 4.5: Reflection Coefficient, Input Impedance, Gain, E-field, H-field, and maximum near E-field of the four antenna structures.

	Anti-Parallel Double Loop	Parallel Double loop	Fractional Helix	Parallel fractional helix
S_{11}	-56.75dB	-58.87 dB	-54.34 dB	-59.50 dB
Z_{in}	17.26i Ω	19.29i Ω	11.85i Ω	20.43i Ω
Gain	-46 dB	-30 dB	-37 dB	-33 dB
E-field (V/m)	82.33	69.68	63.95	89.49
H-field (A/m)	4.61	4.42	4.02	3.78
Max near E total (V/m)	50.81	48.30	12.09	38.75

For this reason, we found it important to focus on the quantity $|B^2|$, since it is a measure of the radiated power, and its value gives an idea about how strong is the power radiated into the Pyrex tube where the plasma is being generated. Hence, one way of

comparison between different antenna structures, is to compare the value of $|B^2|$, because a higher $|B^2|$ means a higherI^2, and thus a higher radiated power.

The magnitudes of $|B^2|$ for the four antenna structures under investigation are plotted in Fig. 47 as a function of the axial distance, and a blue window is added to show where exactly the antenna is being placed. This is done to witness if there is a correlation that can relate the magnitude of $|B^2|$ to the power coupling efficiency of the antenna, and the plasma generation.
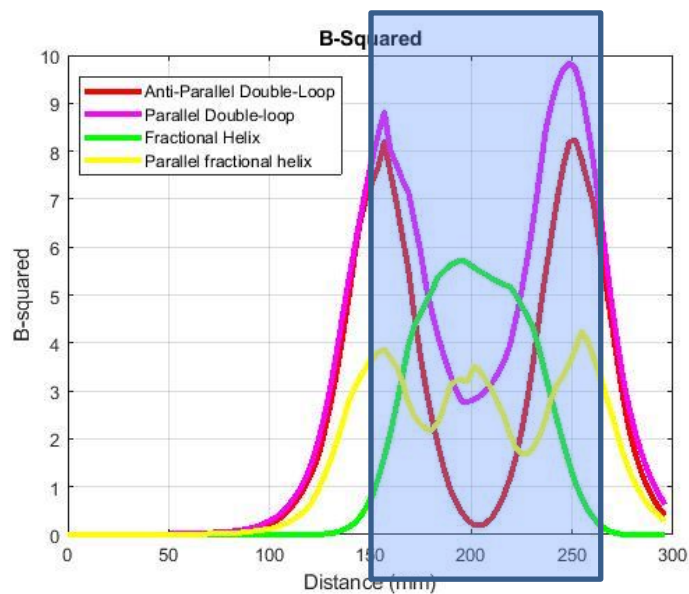
Figure 47: Magnitude of $|B^2|$ as a function of axial distance for the four antennae

For a detailed comparison amongst the four antennas, a new experiment run was launched, and four different scans were acquired. It is important to point out here that the four antenna configurations are kept within the same conditions and are wound symmetrically around the Pyrex tube where the plasma is generated. The antennas are tested under the same exact external conditions, with an external magnetic field of 300

mAmps, input power of 1 kW, and a gauge pressure of 2.37 mTorr. The scans are conducted at perfect matching conditions; that is, the reflected power at the power supply is minimal.

It is obvious in Fig.48 that the parallel double loop antenna was capable of attaining the highest values of plasma densities, with an average value of $14.2138 \times 10^{18}m^{-3}$ calculated between 2 cm and 2.3 cm probe positions. This was followed by the parallel fractional helix antenna attaining an average electron density of $11.8494 \times 10^{18}m^{-3}$, then comes the fractional helix with $6.6616 \times 10^{18}m^{-3}$ average electron density, and finally the anti-parallel double loop which generated the minimal electron density values with an average of $1.2764 \times 10^{18}m^{-3}$.
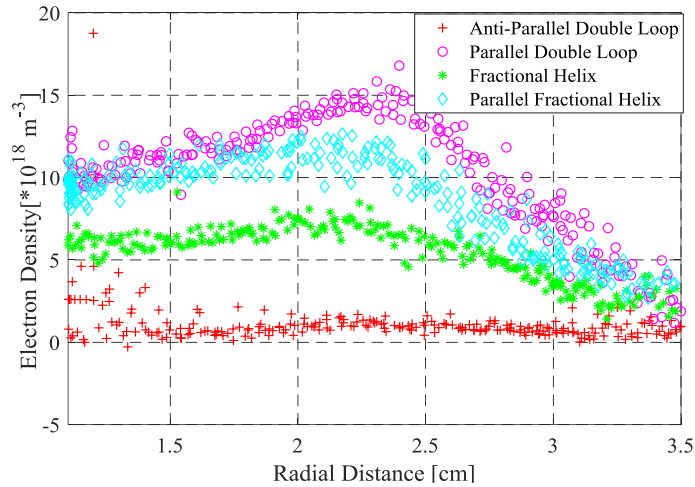
Figure 48: Electron density vs. radial distance for the four antenna structures

D. Conclusion

Amongst all the parameters generated for the tested antennas via simulation, the realized gain was the only parameter whose enhancement is proven to correlate with the

improved energy coupling and higher density plasma generation as shown in Fig. 49. The maximum realized gain values of the four antennas under experimentation had the same increasing order as the one followed by the electron density. That is; the parallel double loop antenna which has the highest gain value generated the highest electron density inside the Pyrex tube, and thus had the best performance. On the other side, the anti-parallel double loop antenna characterized with the lowest value of the realized gain, generated the lowest electron density. This helps us deduce that employing an antenna with higher gain values in a helicon plasma device improves the performance of the helicon system and increases the power deposition into the plasma and thus the electron density values.
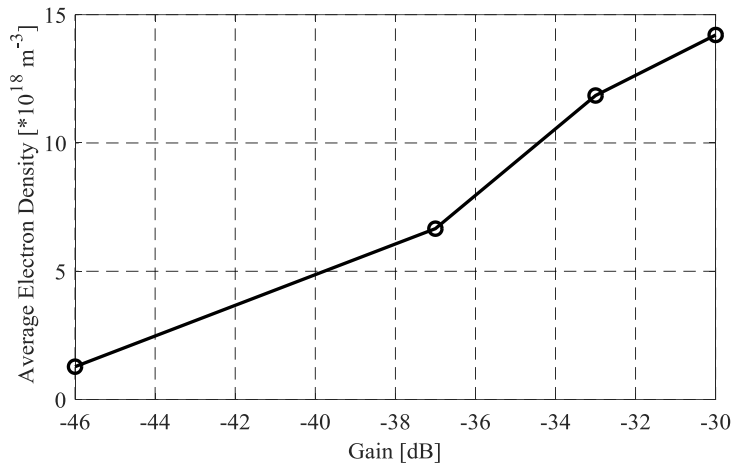
Figure 49: Average electron density vs. realized gain of the antenna

CHAPTER V

A NEW ANTENNA DESIGN FOR A HIGHER ELECTRON DENSITY

A. Objective and Problem Statement

Based on the conclusion drawn from the previous chapter, and in order to correlate the gain enhancement with the improved energy coupling and higher density plasma generation, a new antenna design is proposed. The main goal behind this section is proposing an antenna design that has a gain larger than that of the routinely used RF antenna structures in plasma generation. The proposed antenna design must increase the efficiency of power coupling into the plasma and increase the density of plasma generated as much as possible. In order to achieve our purpose, the design started from an 11 turn helical antenna and then evolved to reach the proposed design.

B. Simulating an 11-turn Helical Antenna

In this part, a helical antenna with N=11 turns is designed and simulated as shown in Fig.50, and the desired observable quantities are determined to verify whether or not the helix is functional at the operating frequency 13.56 MHz. The antenna is considered a miniaturized helix antenna since it has a radius of 4.5 cm which is significantly smaller than the wavelength at the operational frequency in free space. The 11 turn helical antenna is modeled and simulated, as shown in figure 51, at the operational frequency f=13.56 MHz. The pitch separating each two turns of the helix is equal to 1.42 cm.
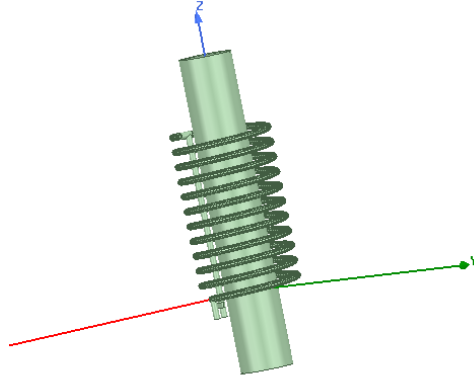
Figure 50: 11 turn helical antenna

The helix is well matched at the frequency of operation f=13.56 MHz, as shown in Fig. 52. The helical antenna reaches a realized gain of magnitude -6.24 dB with an omnidirectional radiation pattern as shown in Fig. 53.

To achieve a high gain, the aperture of a helical antenna needs to be comparable to its wavelength. For this design, the wavelength in free space corresponding to the frequency of operation is $\lambda = \frac{c}{f} = \frac{3 \times 10^8}{13.56 \times 10^6} = 22.12\ m$. However, the radius of the modeled helix a= 4.5 cm is significantly smaller than the wavelength $(\sim \lambda/500)$ in free space. This justifies the negative gain of the antenna. It is important to note here that the realized gain value of the helix resembles an antenna property in its far field and not in the near field where plasma is being generated.
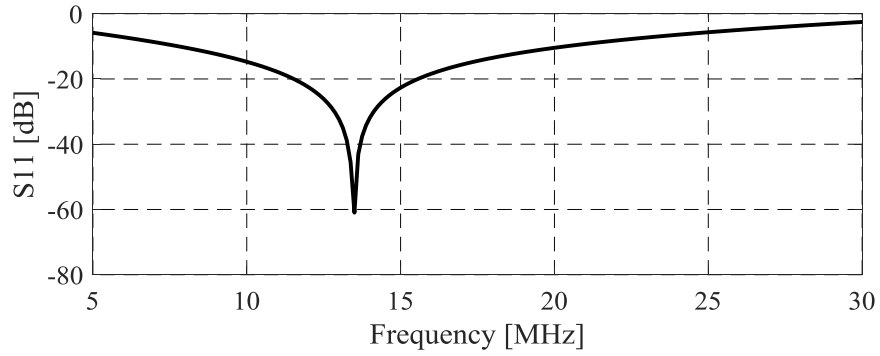
Figure 50: S11 parameter for the 11 turn helix
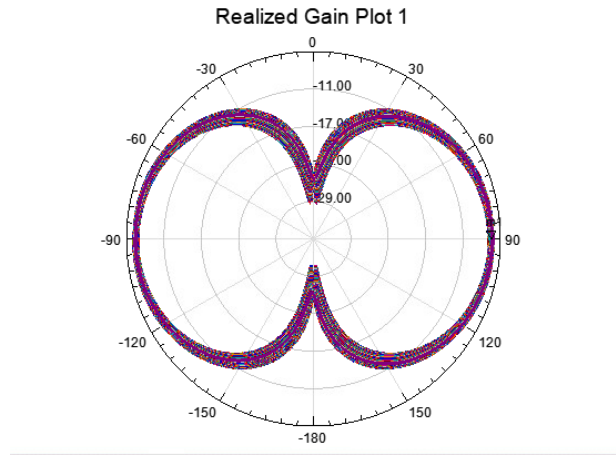
Figure 51:2D gain plot for the 11 turn helix

C. Proposed Structure

The modeling of an 11- turn helix antenna revealed higher gain in comparison to the anti-parallel double loop, parallel double loop, fractional helix, and parallel fractional helix antennas. For this reason, the new antenna structure proposed in this chapter is based on the helical geometry. Before implementing the design, all constraints forced by the plasma device dimensions were taken into consideration. The upper limit of the radius of the antenna design is 10 cm due to the presence of a 4 inch outer cylinder. The lower limit of the radius is set to 2.5 cm which is the radius of the Pyrex cylindrical tube around

which the antenna will be wrapped. Therefore, the antennas radius was chosen to be 1 cm greater than that of the Pyrex tube. In addition, the length of the antenna is restricted by the length of the Pyrex tube to 15 cm.

According to antenna theory [25], a quadrifilar helical antenna has a realized gain that is greater than the conventional helical antenna [26]. For this reason, the antenna was designed based on both the helix and the Quadrifilar helix' conventional structures as shown in Fig. 54. It is composed of five helices. Four of these helices are arranged in a quadrifilar geometry and connected from their upper end to the fifth helix. The proposed antenna design comprises of the following specs:

✓ The five helices have a radius a= 3.5 cm, which is 1 cm greater than the radius of the cylindrical tube which is equal to 2.5 cm.

✓ The four helices building the quadrifilar helix are almost one turn helices (one of them is exactly one turn and the other three increase gradually to intersect the upper helix).

✓ The pitch of the four helices building the quadrifilar helix is equal to 8 cm.

✓ The fifth helix is a three turn helix with a pitch equal to 1.42 cm.

✓ The operational frequency is 13.56 MHz.

✓ The helix arms are with a rectangular geometry for an easier fabrication using laser cutting techniques.

✓ The rectangular strips forming each helix have a width w= 3 mm and a height h=1 cm to be able to mount the cooling pipes on each of them.
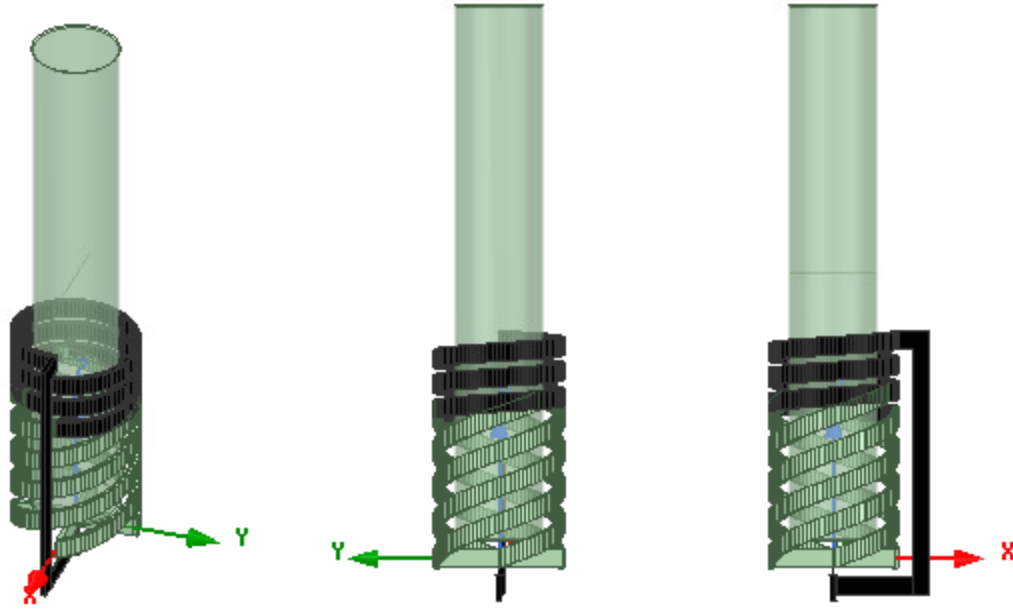
Figure 52: Side Views of the Proposed Antenna Structure

D. Simulation Results

The antenna design is modeled and simulated using AED simulator, and the main desirable quantities are generated by the software at the operational frequency f= 13.56 MHz. The cross shape joining the four helices of the quadrifilar is connected at its center to the central pin of the coax, however; the upper terminal of the three turn helix is connected to the outer pin of the coax which is connected to ground. The magnitude of the S_{11} parameter at the resonant frequency is -50.76 dB, as shown in Fig. 55. This ensures great impedance matching of the input impedance of the antenna, which is equal to 0.00+48.66j Ω , as shown in Fig. 56. It is important to note here, that this antenna is designed to be matched to 48.66j Ω and not to 50Ω. Hence, a matching network will be placed between this antenna and the power supply in order to match it to 50Ω .

57
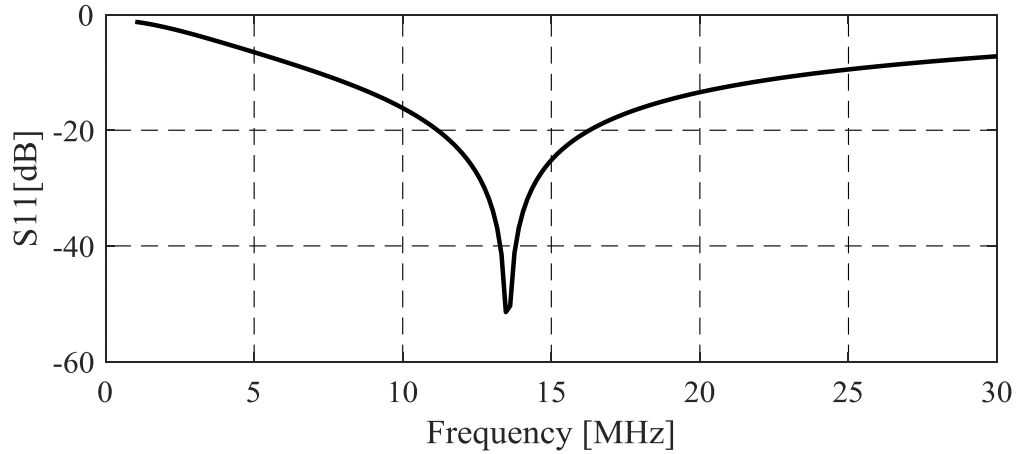
Figure 53: S11 parameter of the proposed antenna structure
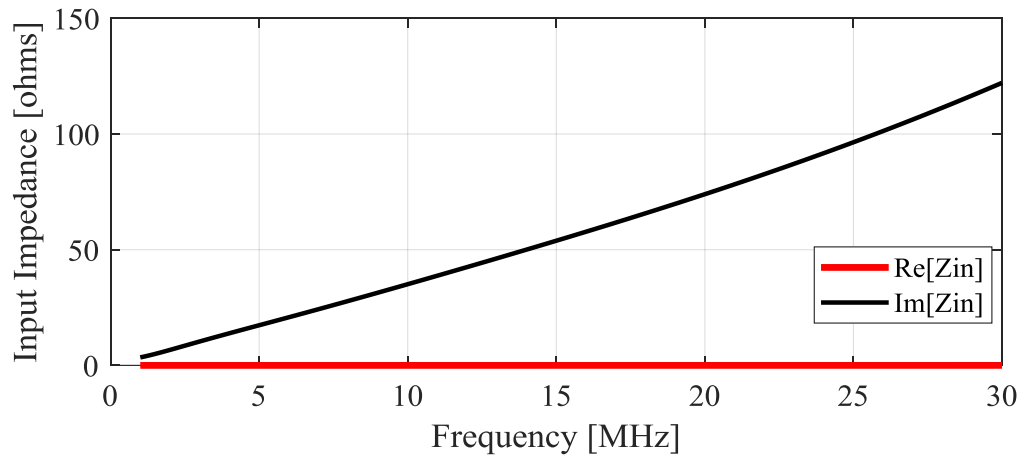
Figure 54: Input impedance of the proposed antenna

In addition, it is significant to point out, that the positive imaginary part of the antenna's input impedance confirms the fact that the employed antenna couples the RF power inductively into the plasma. The bandwidth of operation of the antenna is determined to be equal to 16.91 MHz from 7.09 MHz to 24.00 MHz as shown in Fig. 56. The 2D and 3D gain plots are shown in figures 57. The radiation pattern of the proposed

antenna design is omnidirectional with a maximum gain equal to -22.83 dB as shown in Figs. 26.
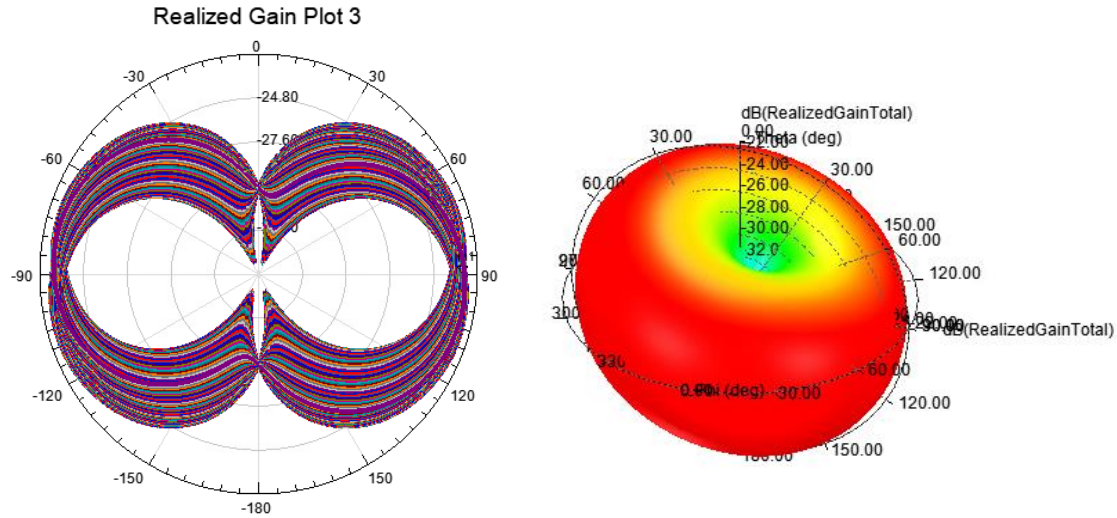
Figure 55: 2D and 3D gain plots of the proposed antenna structure

E. Experimentation Leading to Modification in the Proposed Antenna Structure

The proposed antennas structure was modeled in 2D using cad tools, printed on a copper sheet of thickness 3mm, fabricated using conductive laser cutting techniques, and finally folded using a rounding machine. The fabricated structure is shown is Fig.58.

The fabricated antenna was wrapped around the Pyrex dielectric tube and tested; however; the antenna was not capable of generating plasma inside the dielectric column, and that was due to the huge mismatch between the antenna input impedance and the impedance of the RF power supply.

Figure 56: Proposed antenna fabricated structure

To make this point clear, it is important to note that seeking an efficient power deposition into the discharge, necessitates the presence of a matching network through which the power supply feeds the antenna with energy. In the Polaris Helicon device used for experimentation, the AM-20 matching network setup is used, which is an L configuration capable of wide range tuning. This matching network setup constitutes of two variable vacuum capacitors, one connected in shunt to handle the loading and the other connected in series to handle the tuning, in addition to a fixed coil.

Upon testing the fabricated antenna structure on the Polaris device, it was deduced that the antenna input impedance falls outside the range of impedances that the AM-20 matching network is capable of tuning. For this reason, the proposed antenna structure with input impedance Z_{in}=0.00+48.66j Ω, was modified to have an input impedance that falls in the range of the input impedances of the four antenna designs that

were tested on the Polaris devise and were successfully matched to the power supply through the AM-20 matching network. To attain this, the upper three turn helix that is connected to the upper part of the quadrifilar helix, was reduced to a one turn helix, as shown in Fig.59, resulting with the modified helix antenna that has an input impedance Z_{in}=0.00+14.0821j Ω. This value of input impedance, shown in Fig.60, falls in the range of input impedances that can be tuned by the available matching network. The simulation parameters were verified for the modified helix antenna, and the antenna was well matched at the desirable frequency of operation f=13.56 MHz, as shown in Fig.61.
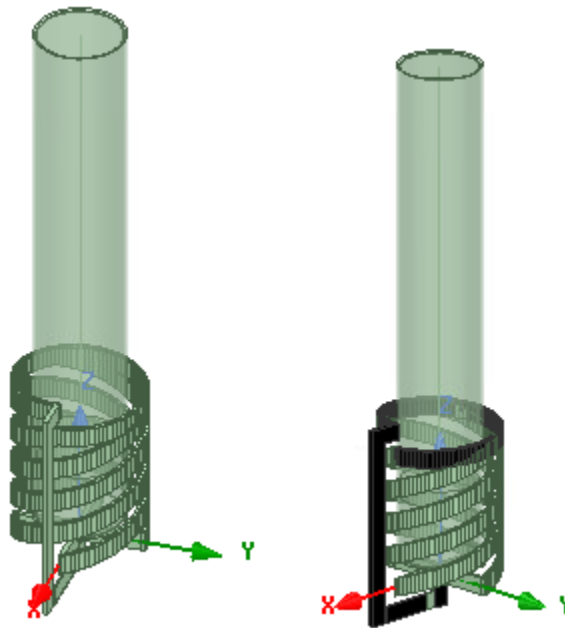
Figure 57: Modified helix antenna
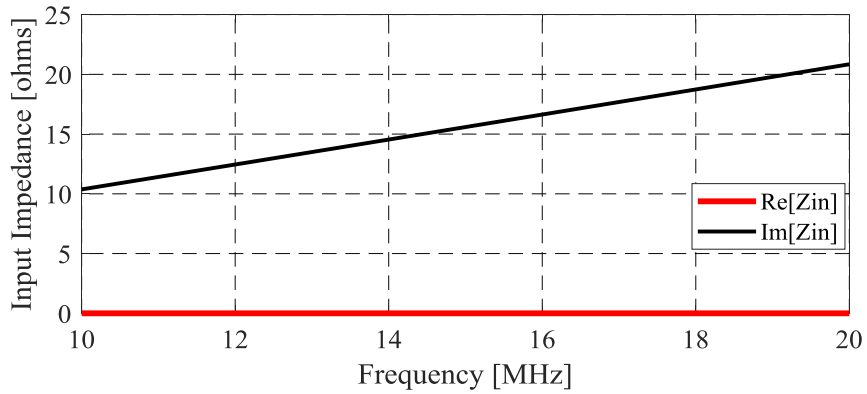
Figure 58: Input impedance of the modified helix antenna
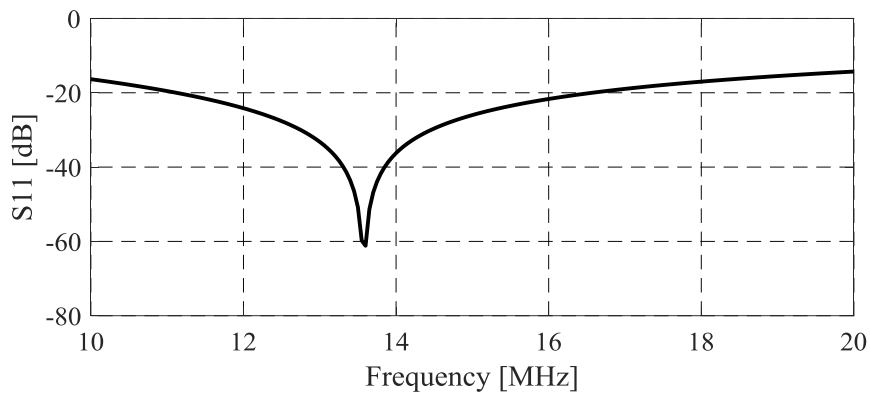
Figure 59: S11 coefficient of the modified helix antenna

The 3D realized gain plot of the proposed antenna geometry is shown in Fig.62. The antenna's radiation pattern is omnidirectional with a maximum gain equal to -27.5 dB. This is greater from the gain values of the four antenna configuration tested previously, and thus we expect that employing this antenna on the Polaris plasma device would help attain plasma density values greater from those obtained by employing any of the previous antenna designs. Moreover, the modified helix antenna radiates in an

omnidirectional pattern in the azimuthal plane rather than radiating in the axial plane. This enhances the electric fields in the azimuthal direction.
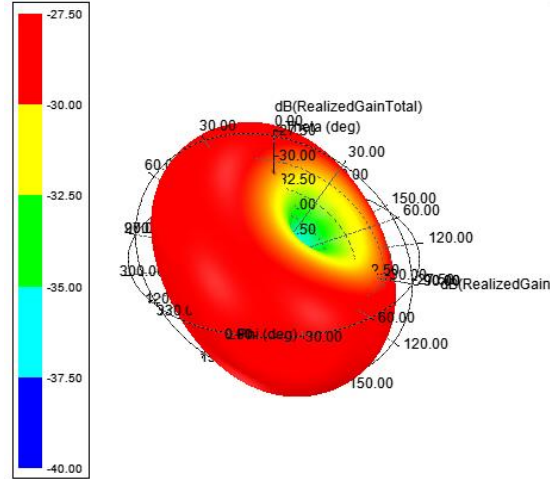
Figure 60: 3D radiation pattern of the modified helix antenna

F. Experimentation of the Modified Helix Antenna

1. Experimental Procedure

The final structure of the proposed antenna design, the modified helix antenna shown in Fig.63, was symmetrically wrapped around the plasma column of the Polaris helicon plasma device as shown in Fig.64, in order to take a look at the overall plasma profile of this plasma source. The experimentation allowed acquiring data through the available diagnostic tool, called the Langmuir probe, which is inserted into the plasma column.

Twelve experimental scans were acquired for the modified helix antenna under testing, and were referred to as the BP scans. These BP scans allow us to identify the

conditions under which a transition from Blue to Pink Mode occurred in the plasma, and help us figure out the settings to maintain a sustainable blue mode. All of this allow us to increase the electron density inside the plasma column and thus make the blue mode reproducible. The twelve BP scans, along with the external conditions under which they were acquired, are summarized in Table.6.1.

Figure 61: Modified helix fabricated antenna

Figure 62: Modified helix antenna mounted on AUB's Lebanese Linear Plasma Device (Polaris)

Table 6.1: Experimental scans of the modified helix antenna

Scan	B(mA)	P(mTorr)	SCCM	P_{in}(W)	P_{ref}(W)
1	350	2.3	15	200	0
2	350	2.3	15	240	0
3	300	1.53	12	500	2
4	300	1.53	12	540	2
5	300	1.51	12	600	3
6	300	1.51	12	640	4
7	300	1.48	12	700	4
8	300	1.47	12	740	8
9	300	1.45	12	800	8
10	300	1.45	12	860	8
11	300	1.42	12	920	8
12	300	1.42	12	1000	8

2. *Discussion*

For a valid comparative analysis, the experimentation of the modified helix antenna structure was performed under the exact external parameters under which the experimentations of the four previous antennas were conducted. As shown in Fig. 67, the modified helix antenna was capable of attaining plasma electron densities significantly higher that the densities achieved by the four antennas with lower realized gain value. This antenna attained an average electron density of $23.9034 \times 10^{18} m^{-3}$, much greater than the average electron density value achieved by the parallel double loop antenna, $14.2138 \times 10^{18} m^{-3}$, which was the best performing antenna amongst the previous four experimented configurations. This reassures the conclusion drawn in the previous section, which states that antennas with higher realized gain values are the antennas capable of generating denser plasma. In addition to this, it is worth emphasizing that the modified helix antenna generates electric fields that radiate in an omnidirectional pattern in the azimuthal plane. This enhances the excitement of the azimuthal mode number m in the helicon wave scheme and thus enhances power deposition by the antenna into the plasma.

Fig.65 and Fig.66 show the electron density and electron temperature plots of the modified helix antenna, respectively, as a function of the radial position, inside the plasma column.
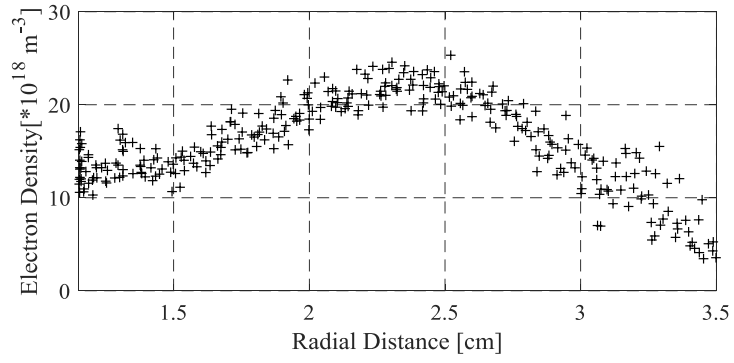
Figure 63: Electron density vs. radial distance of the modified helix antenna
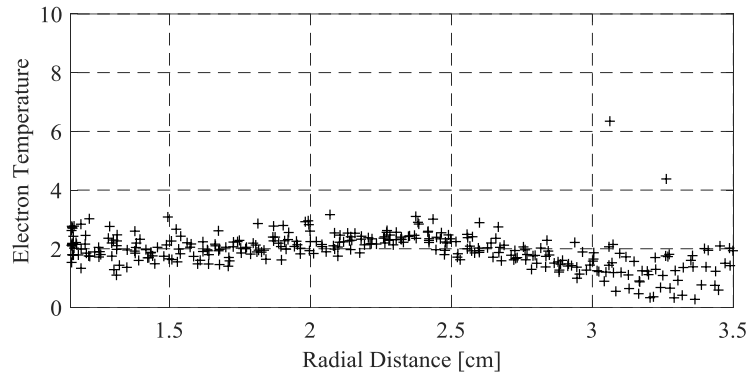
Figure 64: Electron temperature vs. radial distance of the modified helix antenna
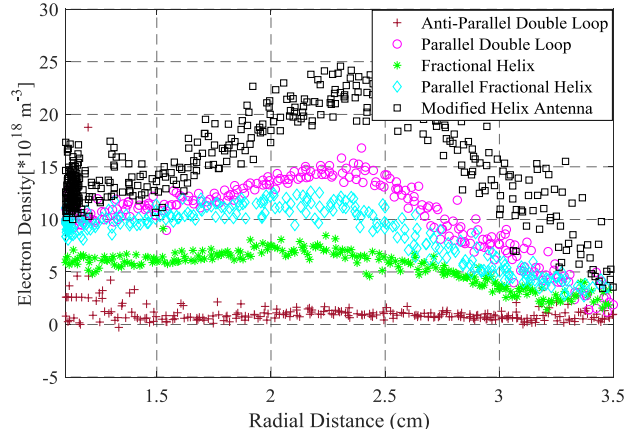
Figure 65: Electron density vs the radial distance of the five antenna structures

Figure 66: Blue mode plasma generation by the modified helix antenna installed on Polaris

3. Conclusion

The proposed design, which is a modified helix antenna, that was designed and experimental validated. Once installed on Polaris, it attained an average electron density that is much greater than the average electron density value achieved by the parallel double loop antenna, the best performing antenna amongst the four experimented structures. This reassures the conclusion drawn in our comparative analysis, which states

68

that antennas with higher realized gain values are the antennas capable of generating denser plasma. Fig.68 validates our hypothesis and correlates the gain enhancement with the improved energy coupling and higher density plasma generation.

Figure 67: Average electron density as a function of the realized gain of an antenna

CHAPTER VI

CONCLUSIONS AND FUTURE WORK

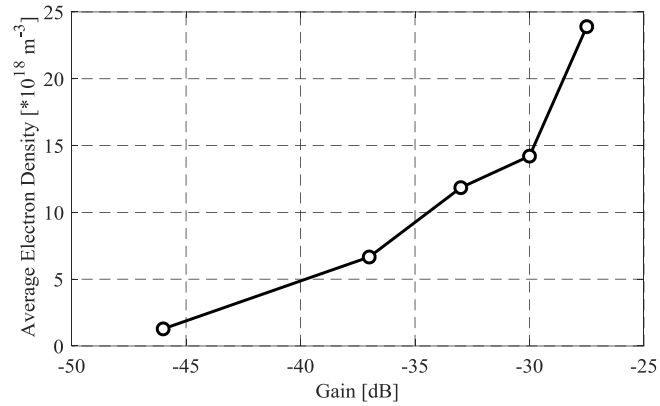Helicon plasma sources are known for their high efficiency in depositing electromagnetic power and producing plasma with high densities. Being a significant part of a helicon plasma device, the antenna which couples the RF power into the plasma and drives the discharge should be designed with high consideration so that the power deposited into the plasma is optimized.

In order to establish a relationship between the properties of an antenna and its power deposition capabilities, we conduct a comparative analysis amongst four commonly used antenna structures in helicon plasma generation. The comparison was based on the parameters characterizing an antenna such as the gain, input impedance, E-field, H-field, and the maximum near E-field. The antennas were also experimented on the Lebanese linear plasma device (Polaris) to assess their performance.

Based on the simulation and experimental results; the realized gain was the only parameter whose enhancement seems to correlate with the improved energy coupling and higher density plasma generation. To validate this investigative relation, a new antenna design with a realized gain value greater than the previous antennas was proposed. The proposed antenna structure is a modified helix antenna that was experimentally tested on Polaris and attained an average electron density that is much greater than the average electron density value achieved by any of the antennas experimented previously. This reassures the conclusion drawn in our comparative analysis, which states that antennas with higher realized gain values are the antennas capable of generating denser plasma.

The work done in this thesis opens the door to experimentation and implementation of various antenna designs with enhanced parameters to find out what techniques help generate plasma with higher densities. This could include quantitative analysis of the effectiveness of the shielding surrounding the antenna on the plasma generation and electron densities. This allows design optimization of the RF system of a helicon plasma source

REFERENCES

[1] Shinohara, S., et al. "Large-area high-density helicon plasma sources." *Plasma Sources Science and Technology* 19.3 (2010): 034018.

[2] Soltani, Behrooz, and Morteza Habibi. "Development of a helicon plasma source for neutral beam injection system of the Alborz tokamak." *Journal of Fusion Energy* 36.4-5 (2017): 152-160.

[3] Scime, E. E., A. M. Keesee, and R. W. Boswell. "Mini-conference on helicon plasma sources." *Physics of Plasmas* 15.5 (2008): 058301.

[4] Melazzi, D., and V. Lancellotti. "A comparative study of radiofrequency antennas for Helicon plasma sources." *Plasma Sources Science and Technology* 24.2 (2015): 025024.

[5] Tarey, R. D., B. B. Sahu, and A. Ganguli. "Understanding helicon plasmas." *Physics of Plasmas* 19.7 (2012): 073520.

[6] Ellingboe, A. R., and R. W. Boswell. "Capacitive, inductive and helicon-wave modes of operation of a helicon plasma source." *Physics of Plasmas* 3.7 (1996): 2797-2804.

[7] Lieberman, Michael A., and Alan J. Lichtenberg. *Principles of plasma discharges and materials processing*. John Wiley & Sons, 2005.

[8] Boswell, Roderick William. "Very efficient plasma generation by whistler waves near the lower hybrid frequency." *Plasma Physics and Controlled Fusion* 26.10 (1984): 1147.

[9] Chen, Francis F. "Plasma ionization by helicon waves." *Plasma Physics and Controlled Fusion* 33.4 (1991): 339.

[10] Lehane, J. A., and P. C. Thonemann. "An experimental study of helicon wave propagation in a gaseous plasma." *Proceedings of the Physical Society* 85.2 (1965): 301.

[11] Lehane, J. A., and F. J. Paoloni. "The propagation of non-axisymmetric Alfvén waves in an argon plasma." *Plasma Physics* 14.7 (1972): 701.

[12] Blevin, H. A., and P. J. Christiansen. "Propagation of helicon waves in a non-uniform plasma." *Aust. J. Phys* 19.501 (1966).

[13] Ferrari, R. L., and J. P. Klozenberg. "The dispersion and attenuation of helicon waves in a cylindrical plasma-filled wave-guide." *Journal of Plasma Physics* 2.2 (1968): 283-289.

[14] Degeling, A. W., et al. "Plasma production from helicon waves." *Physics of Plasmas* 3.7 (1996): 2788-2796.

[15] R.W Boswell, Chapter 3 - Theory of- Helicon Wave Propagat.

[16] Stratakos, Yorgos, Angelos Zeniou, and Evangelos Gogolides. "Comparison of helical and helicon antennas as sources of plasma excitation using a full wave 3D electromagnetic analysis in vacuum." *Plasma Processes and Polymers* 14.4-5 (2017): 1600107.

[17] Shamrai, Konstantin P., V. P. Pavlenko, and V. B. Taranov. "Excitation, conversion and damping of waves in a helicon plasma source driven by an m= 0 antenna." *Plasma physics and controlled fusion* 39.3 (1997): 505.

[18] Shinohara, S., T. Tanikawa, and T. Motomura. "A segmented multi-loop antenna for selective excitation of azimuthal mode number in a helicon plasma source." *Review of Scientific Instruments* 85.9 (2014): 093509.

[19] Light, Max, and Francis F. Chen. "Helicon wave excitation with helical antennas." *Physics of Plasmas* 2.4 (1995): 1084-1093.

[20] Thompson, Derek S., et al. "Ion heating and flows in a high power helicon source." *Physics of Plasmas* 24.6 (2017): 063517.

[21] [Online].Available:.https://www.plasmas.org/rot-plasmas.htm

[22] [Online].Available:.https://www.plasmatreat.com/plasma-technology/what-is-plasma.html

[23] Shinohara, Shunjiro. "Helicon high-density plasma sources: physics and applications." *Advances in Physics: X* 3.1 (2018): 1420424.

[24] Chen, Francis F. "Helicon discharges and sources: a review." *Plasma Sources Science and Technology* 24.1 (2015): 014001.

[25] Balanis, Constantine A. *Antenna theory: analysis and design*. John wiley & sons, 2016.

[26] Slade, Bill. "The basics of quadrifilar helix antennas." *Orban Microwave Inc., Orlando, FL, USA* (2015).